



Review

Green Production of Biomass-Derived Carbon Materials for High-Performance Lithium–Sulfur Batteries

Chao Ma ¹, Mengmeng Zhang ², Yi Ding ², Yan Xue ^{1,*}, Hongju Wang ³, Pengfei Li ^{2,*} and Dapeng Wu ^{2,*}

¹ College of Mechanical and Electrical Engineering, School of 3D Printing, Xinxiang University, Xinxiang 453003, China

² School of Business, Henan Normal University, Xinxiang 453007, China; lipengfei@htu.edu.cn (P.L.)

³ Key Laboratory for Yellow River and Huai River Water Environmental and Pollution Control, School of Environment, Ministry of Education, Collaborative Innovation Center of Henan Province for Green Manufacturing of Fine Chemicals, Henan Normal University, Xinxiang 453007, China

* Correspondence: xueyan6066@163.com (Y.X.); dapengwu@htu.edu.cn (D.W.)

Abstract: Lithium–sulfur batteries (LSBs) with a high energy density have been regarded as a promising energy storage device to harness unstable but clean energy from wind, tide, solar cells, and so on. However, LSBs still suffer from the disadvantages of the notorious shuttle effect of polysulfides and low sulfur utilization, which greatly hinder their final commercialization. Biomasses represent green, abundant and renewable resources for the production of carbon materials to address the aforementioned issues by taking advantages of their intrinsic hierarchical porous structures and heteroatom-doping sites, which could attribute to the strong physical and chemical adsorptions as well as excellent catalytic performances of LSBs. Therefore, many efforts have been devoted to improving the performances of biomass-derived carbons from the aspects of exploring new biomass resources, optimizing the pyrolysis method, developing effective modification strategies, or achieving further understanding about their working principles in LSBs. This review firstly introduces the structures and working principles of LSBs and then summarizes recent developments in research on carbon materials employed in LSBs. Particularly, this review focuses on recent progresses in the design, preparation and application of biomass-derived carbons as host or interlayer materials in LSBs. Moreover, outlooks on the future research of LSBs based on biomass-derived carbons are discussed.

Keywords: carbon materials; biomass; working mechanism; lithium–sulfur batteries; cathodes; interlayer



Citation: Ma, C.; Zhang, M.; Ding, Y.; Xue, Y.; Wang, H.; Li, P.; Wu, D. Green Production of Biomass-Derived Carbon Materials for High-Performance Lithium–Sulfur Batteries. *Nanomaterials* **2023**, *13*, 1768. <https://doi.org/10.3390/nano13111768>

Academic Editor: Diego Cazorla-Amorós

Received: 1 April 2023

Revised: 10 May 2023

Accepted: 16 May 2023

Published: 30 May 2023



Copyright: © 2023 by the authors. Licensee MDPI, Basel, Switzerland. This article is an open access article distributed under the terms and conditions of the Creative Commons Attribution (CC BY) license (<https://creativecommons.org/licenses/by/4.0/>).

1. Introduction

Nowadays, human society is facing more and more critical social problems as it is confronted with the ever-growing energy demands and serious environmental crises. In order to efficiently store clean and renewable energy, such as solar, wind, tide, geothermal and other energy sources for sustainable development, research studies on advanced energy storage systems have attracted intense attention worldwide [1–6]. Among them, secondary batteries with a high energy density represent a cutting-edge energy storage technology. Traditional lithium batteries, which adopt graphite as the anode material and lithium metal oxide (LiCoO₂, LiNi_xCo_yMn_{1-x-y}O₂) or lithium phosphate (LiFePO₄) as the cathode material, demonstrate a theoretical energy density of 400 Wh kg⁻¹, which has been widely used in portable electronic devices. After years of research and development, the electrochemical properties of the electrodes of lithium-ion batteries have been reaching their theoretical values, but this still cannot fully meet the needs for energy storage devices to power electric vehicles or to store the huge volume of electricity generated from clean-energy harnessing facilities.

Therefore, researchers have turned their attention to other cathode materials with a high theoretical capacity. Among various potential cathode materials, lithium–sulfur

batteries (LSBs) have attracted much attention as a potential low-cost and efficient energy storage system due to the advantages of high theoretical capacity (1675 mAhg^{-1}), high energy density (2600 Whkg^{-1}), wide sources and low cost of elemental sulfur [7,8]. LSBs consist of elemental sulfur as the cathode, an electrolyte, a separator and lithium metal as the anode. Through the multi-electron electrochemical conversion between sulfur and lithium, LSBs could give rise to a much higher specific capacity than that of traditional lithium batteries.

Carbon-based materials represent a group of important raw materials for different industries. Due to their high electroconductivity and high thermal and chemical stability, as well as bio-compatibility, many types of carbon materials, such as graphene or reduced graphene oxides [4–15], carbon fibers [16–18], carbon dots [19], active carbons [20–22] and biomass-derived carbons [23–32], have been deliberately prepared for different application aims. Biomass has many definitions, such as biodegradable products, wastes and residues from agriculture, forestry and related industries, including fisheries and aquaculture, as well as biodegradable parts of industrial and municipal wastes. In addition, biomass is also regarded as a class of organic macromolecular materials derived from organisms [33]. During carbon preparation, biomass precursors undergo thermochemical transformation under high-temperature conditions, which could be classified into two distinctive processes. The first one is solid-state carbonization, which represents the decomposition of biomass precursors under a high temperature and an inert atmosphere to generate carbon-rich and thermal stable products [34]. The second one is hydrothermal carbonization, which could convert wet biomass into a carbon-rich product (hydrochar). In these processes, the organic components in the biomass experience drastic chemical changes, such as carbon skeleton recombination and functional group decomposition, which finally yield a carbon atom network with high-conductivity sp^2 domains and rich surface functional groups [34]. Generally, activation processes are introduced to further treat the as-obtained carbon materials to increase the surface area and to regulate the pore structures. These activation processes are usually carried out under high-temperature conditions and with the assistance of physical (water vapor or carbon dioxide) or chemical activators (KOH, H_3PO_4 , ZnCl_2 , NaOH, etc.) [35,36]. In addition, the templating method is also one of the commonly used strategies to optimize the surface area and pore structures of as-obtained carbon materials. Generally, templates are firstly introduced into a biomass precursor, which is then carbonized under a high temperature with inert atmosphere. Finally, the templates are removed by immersion in a NaOH or HF solution to generate carbon materials with ordered pore distribution [37].

Activated carbon production from biomass has long been regarded as important research in materials science. At the very beginning, biomass-activated carbon was only used for adsorption. Thanks to their rich pore structures, huge specific surface area, and good physical and chemical stability, biomass-derived carbon materials have gradually developed into a wide range of adsorbents for application in purification, deodorization, decolorization and separation [38]. China is a traditional agricultural country, and there are abundant biomasses produced from agriculture, forestry, animal husbandry and aquaculture annually. In addition, illegally discarded or wrongly treated biomass has become an important source that causes environmental pollution. Therefore, the production of functional carbon materials from biomass could not only lead to economic benefits but also alleviate such environmental problems, which has attracted more and more attention.

At present, biomass-derived carbon materials are employed in energy storage applications, such as supercapacitors [39], lithium-ion batteries [40,41], lithium–sulfur batteries (LSBs) [42,43], and so on. As for the application of biomass-derived carbons in LSBs, many review works have been devoted to highlight the significance of these materials from different aspects [44–52]. This review work will focus on discussing recent advancements in the design, preparation and application of biomass-derived carbons as host or interlayer materials in LSBs. Moreover, outlooks on rational preparation based on biomass-derived carbons and potential future research on LSBs are also discussed.

2. Fundamentals

2.1. Working Principles of LSBs

In the discharge curve shown below, two typical discharge platforms at 2.3 and 2.1 V could be clearly observed, corresponding to the solid (S_8), liquid (Li_2S_n) and solid (Li_2S_2/Li_2S) processes, respectively [53] (Figure 1a). S_8 is firstly converted into long-chain Li_2S_n , and then the long-chain Li_2S_n is converted to Li_2S_2/Li_2S . For the higher-voltage discharge platform located at 2.3 V, S_8 is reduced to long-chain polysulfide, corresponding to the theoretical capacity of 418 mAh g^{-1} . For the lower-voltage discharge platform at 2.1 V, polysulfide is further reduced to insoluble Li_2S_2/Li_2S , corresponding to the theoretical capacity of 1254 mAh g^{-1} . During the charging process, 2.3–2.4 V could be regarded as a platform, corresponding to the transformation process from Li_2S_2/Li_2S to S_8 . The intermediate polysulfide dissolves and diffuses into the electrolyte due to the concentration gradients and electric field forces (Figure 1b). In addition, a small polarization voltage can be observed during the initial phase of charging, which is due to the final product of the discharge phase (Li_2S_2/Li_2S) being an insulator, thus leading to a large inter-phase transition barrier.

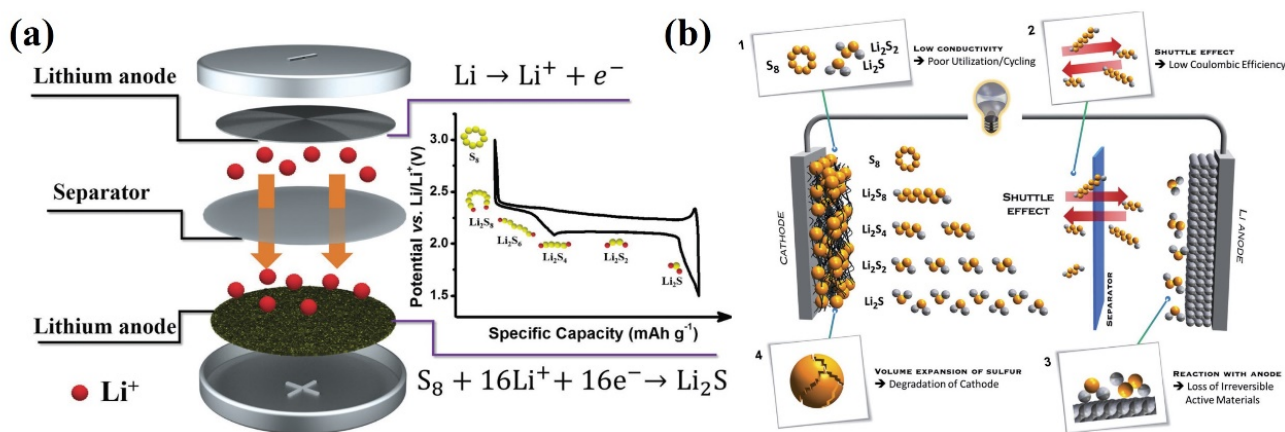


Figure 1. (a) Structure of an LSB and the typical charge–discharge process and intermediate product conversion of the battery [53]. Reprinted with permission from Ref. [53]. Copyright 2018 Wiley-VCH. (b) Conversion of soluble polysulfide and insoluble Li_2S_2/Li_2S during charge and discharge in a secondary lithium–sulfur battery consisting of a sulfur positive electrode and lithium negative electrode [8]. Reprinted with permission from Ref. [8]. Copyright 2017 Wiley-VCH.

2.2. Obstacles for LSBs

Due to their high theoretical capacity and energy density, LSBs have attracted extensive attention from both domestic and overseas researchers. However, LSBs still suffer from various inherent technical bottlenecks as listed below, which greatly restricts their application. The first bottleneck is the insulation of the charge and discharge products. Under room temperature, elemental sulfur (S_8) is an insulator for Li^+ and electrons ($5 \times 10^{-28} \text{ S cm}^{-1}$). Likewise, Li_2S is also an insulator for both Li^+ and electrons ($<10^{-14} \text{ S cm}^{-1}$) [54]. In the working process, the low Li^+ and electron conductivity of the charge–discharge product hinders the charge–discharge process of the battery. When sulfur is used alone as the electrode material, such property leads to two serious problems which restrict the development of lithium–sulfur batteries: the low utilization rate of active substances and the slow reaction kinetics. The intrinsic insulation of S_8/Li_2S severely limits the utilization rate of S active substances, resulting in low capacity and low-rate capacity. Although the solid–liquid reaction with a discharge platform of about 2.3 V has a faster reaction kinetics, it is still difficult to achieve the theoretical capacity. Additionally, previous reports have demonstrated that after multiple cycles, there is still S_8 that is not involved in the reaction. In addition, due to the limited Li^+ and electro-kinetics, in the charge–discharge curve of lithium–sulfur

batteries, a large polarization phenomenon is often observed on the lower discharge platform, which further leads to the attenuation of the actual energy density.

The second bottleneck is the shuttle effect of intermediate products. Due to the transport of Li^+ between the two electrodes, the electrode reaction of lithium–sulfur batteries involves a series of reversible lithiation and delithiation processes. In this series of transformation, the production of soluble Li_2S_n ($n \geq 4$) is inevitable, which leads to a series of negative effects [55]. Due to the concentration gradient, the high-valence polysulfide Li_2S_n ($n \geq 4$) will migrate to the anode, react with lithium metal at the anode, and then generate $\text{Li}_2\text{S}_2/\text{Li}_2\text{S}$. Therefore, during the charge–discharge process, polysulfide cannot completely migrate back to the cathode, which results in an irreversible loss of active materials. Afterward, the continuous deposition of $\text{Li}_2\text{S}_2/\text{Li}_2\text{S}$ on the surface of the lithium negative electrode leads to the continuous generation of solid electrolyte interface film (SEI film) on the anode surface, which hinders the release of Li^+ and the effective contact between the electrolyte and the negative electrode, resulting in a continuous increase in battery impedance with an increase in the number of cycles. As the dissolution and deposition of active substances redistribute after longtime recycles, a passivation layer forms on the surface of the positive electrode material, which greatly increases the surface resistance of the electrode. The production of soluble Li_2S_n ($n \geq 4$) increases the viscosity of the electrolyte and reduces the conduction rate of Li^+ and electrons in the electrolyte, which poses negative impact on the rate capability of the battery. Therefore, due to the severe shuttle effect, a battery can only maintain a limited number of cycles and experiences poor cycle stability, low coulomb efficiency and self-discharge. Because the density difference between S_8 and Li_2S is great, active species of the cathode exhibits a volume expansion of nearly 80% during the discharge process. Such a massive volume expansion leads to two invisible problems. The first one is that the severe volume expansion triggers pulverization and shedding of active materials from the current collector. Meanwhile, the volume expansion also causes a series of safety problems, which seriously limits the practical application of LSBs.

3. Recent Progresses in Carbon Materials for LSBs

As we have stated before, the cathode material of LSBs plays an important role in these storage devices. In order to solve the aforementioned technical bottleneck and realize the commercial production of lithium–sulfur batteries, a large number of scholars have dedicated efforts to optimizing the LSB system from the perspective of cathode materials, hoping to make up for the intrinsic defects of lithium–sulfur batteries based on the design of cathode materials. According to recent research on carbonous cathodes for LSBs, we summarize recent progresses into two categories: structural regulation and heteroatom doping of carbonous materials.

3.1. Structural Regulation of Carbons

Carbon materials exist widely in the natural environment and have stable physical and chemical properties. The introduction of carbon materials can significantly improve the electronic conductivity and ion transport and buffer the volume expansion of active materials, which could avoid the pulverization and shedding of the positive electrode structure in the process of charge and discharge. Therefore, as shown in Figure 2, the exploration of carbon/sulfur composite cathode materials has triggered great research attention, and carbon materials, including porous carbon, hollow carbon structure, graphene, and so on, are commonly used for the cathode in lithium–sulfur batteries [53].

Porous carbon. Porous carbon is a functional carbonaceous material with porous structure. According to the pore size distribution, porous carbons could be classified into microporous carbon materials (pore size less than 2 nm), mesoporous carbon materials (pore size between 2 and 50 nm), macroporous carbon materials (pore size greater than 50 nm), and hierarchical porous carbon materials (with a variety of pore structures). High porosity and high specific surface area are conducive to the storage and uniform distribution of

sulfur. It is also proposed that a porous structure could lead to better inhibition of the dissolution and diffusion of polysulfides, which effectively reduces the shuttle effect and, thus, improves the electrochemical performances of LSBs [47,48].

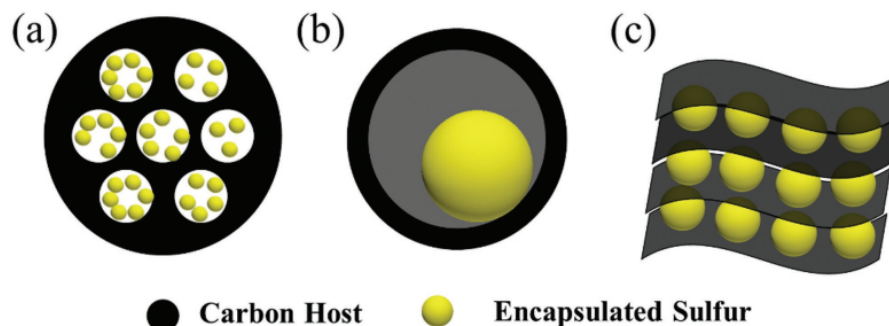


Figure 2. Carbon-based sulfur carriers with different nanostructures: (a) porous structure; (b) hollow structure; and (c) lamellar graphene structure [53]. Reprinted with permission from Ref. [53]. Copyright 2018 Wiley-VCH.

As shown in Figure 3a, sucrose is used as a carbon source to obtain uniform microporous carbon spheres with a specific surface area of $843.5 \text{ m}^2 \text{ g}^{-1}$ and a pore size distribution of mainly 0.7 nm [56]. When the sulfur content is $42 \text{ wt}\%$, the initial discharge capacity could amount to $1183.5 \text{ mAh g}^{-1}$, and after a long period of cycling, it still has a reversible capacity of 650 mAh g^{-1} . The electrode only shows a discharge platform at 1.8 V , which is not a typical lithium–sulfur battery with two discharge platforms, and the high-voltage discharge platform is absent. The unique phenomena could be interpreted as that due to their small size, sulfur molecules are the main species stored in the micropores of the carbon matrix, which avoids the generation of soluble polysulfide and results in a typical charge–discharge curve. As demonstrated by the theoretical simulation (Figure 3b) [7], when the size of microporous carbon is small enough (0.5 nm), S_8 molecules could be split into small sulfur molecules with a short chain length and stored in the micropores, which could inhibit the transformation from S_8 to S_4^{2-} , alleviate the shuttle effect of polysulfides, and, finally, result in the high capacity retention and coulombic efficiency during the charge–discharge process. Highly ordered mesoporous structures with a pore size of $3\text{--}4 \text{ nm}$ are also synthesized as a conductive matrix to accommodate the S loading. During the charge and discharge process, this structure promotes the reaction between Li^+ and sulfur and inhibits the diffusion of soluble polysulfide by trapping polysulfide within the carbon framework [57].

Carbons with hierarchical porosities. Microporous carbon has a high specific surface area, which can ensure the dispersion and contact of elemental sulfur in the conductive matrix. Moreover, the strong physical adsorption capacity of micropores can effectively inhibit the shuttle effect. However, micropores can only provide a limited pore volume, which makes it difficult to accommodate higher active substances. When sulfur loading exceeds the critical amount, the extra sulfur will harm the electrical contact with the conductive matrix, which will reduce the utilization rate of active substances and limit the overall energy density of the battery. Large pores and mesoporous pores can house more sulfur than that of the micropores, which could substantially increase the sulfur loading amount of the electrode and effectively alleviate the volume expansion during the charge and discharge process. However, physical adsorption is not capable enough in inhibiting the dissolution and diffusion of polysulfides, thus resulting in an irreversible loss of active substances. Therefore, the design of hierarchical porous carbon materials with various pore size distributions could well balance the advantages of macroporous, mesoporous and microporous carbon materials and, thus, lead to improved electrochemical performances.

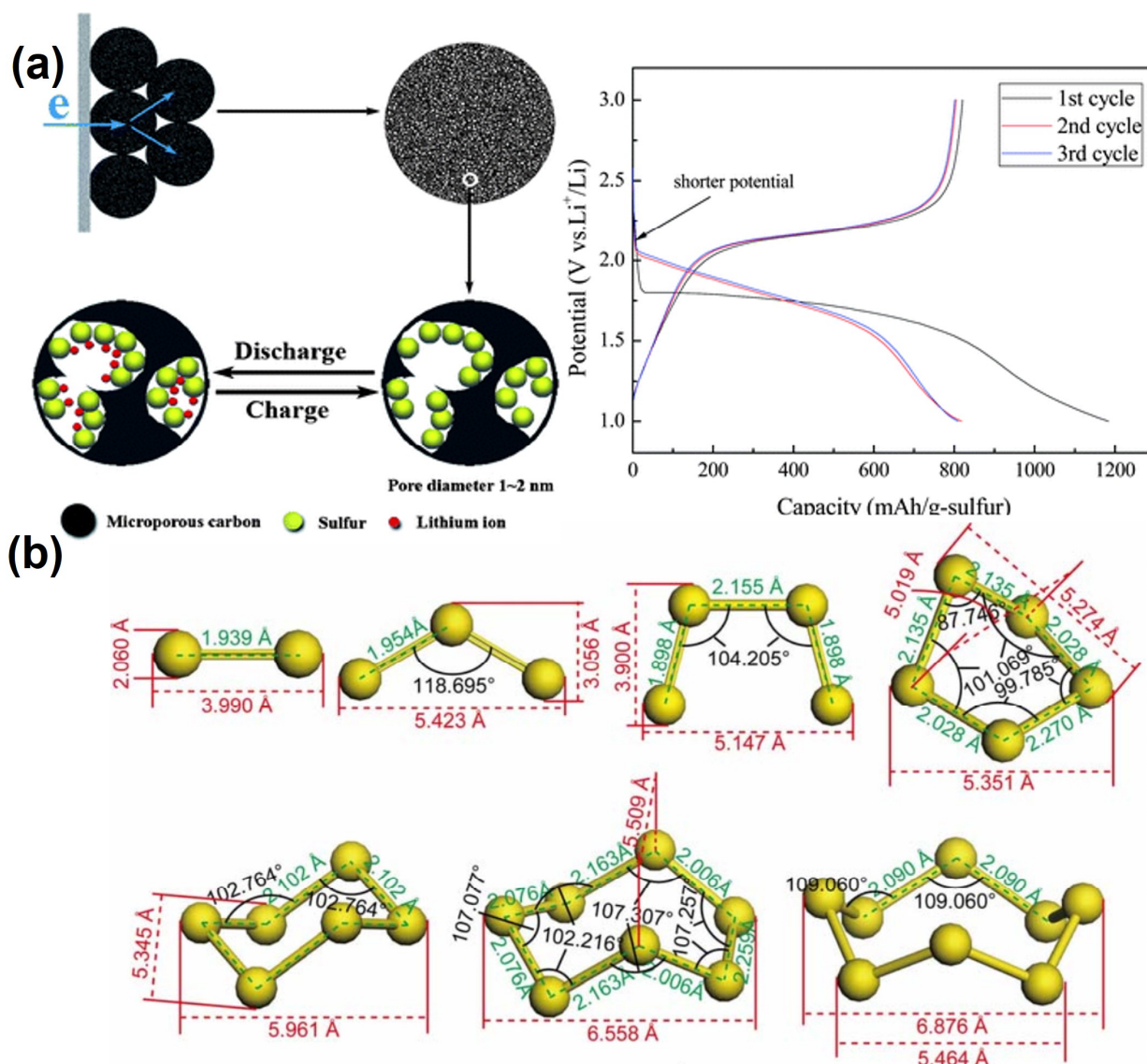


Figure 3. (a) The structure diagram and the discharge curve of microporous carbon spheres [56]. Reprinted with permission from Ref. [56]. Copyright 2008 Royal Society of Chemistry. (b) Models of various polysulfides formed during the charge and discharge process [7]. Reprinted with permission from Ref. [7]. Copyright 2012 American Chemical Society.

Liang et al. used ordered mesoporous carbon as the precursor and KOH as the activator to obtain hierarchical porous carbon with a dual-pore distribution (3 nm and 7.3 nm) (Figure 4a) [58]. Sulfur is found evenly distributed in the conductive carbon matrix, in which the micropores serve as the storage space of active sulfur to ensure the contact between sulfur and the conductive matrix. Mesoporous pores not only could effectively accommodate polysulfides dissolved in the electrolyte but also provide a fast transport channel for lithium ions. In addition, a layer of microporous carbon is coated on the surface of the highly ordered mesoporous structure to obtain a hierarchical porous carbon material with a core–shell structure (Figure 4b) [59]. The ordered mesoporous could greatly improve the sulfur loading amount and make full utilization of the carbon matrix. Meanwhile, the microporous carbon shell could function as a polysulfide barrier to reduce the capacity decay of the battery. Based on this, a rapid spray drying method was adopted to obtain carbon spheres with a hierarchical porous structure (Figure 4c) [60]. Mesoporous and microporous structures could be introduced inside the carbon spheres, which helps to achieve high sulfur accommodation. The outer microporous shell could be used as

a physical site to anchor polysulfides to avoid the irreversible loss of active substances induced by the diffusion of polysulfides.

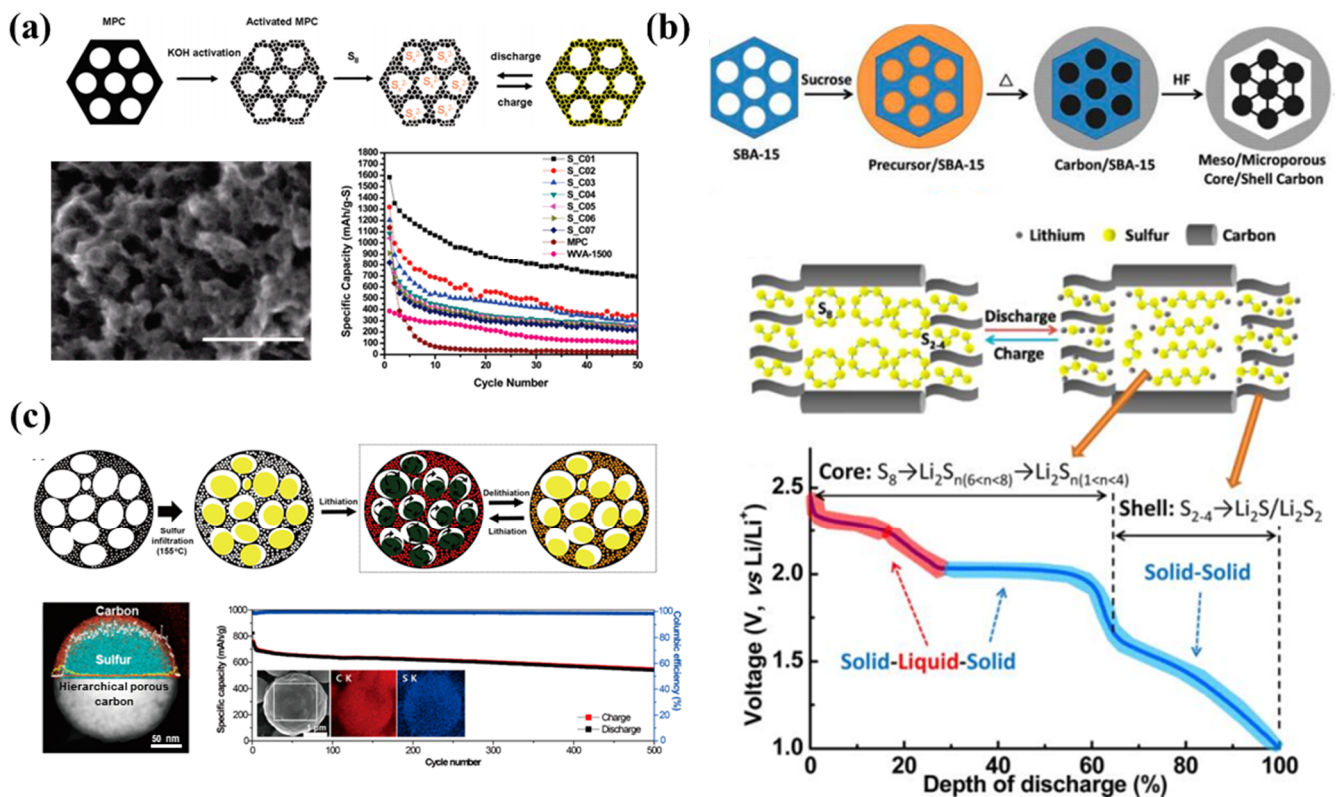


Figure 4. (a) The synthesis route, SEM images and corresponding cycle performance curves of carbon materials with different pore size distributions [58]. Reprinted with permission from Ref. [58]. Copyright 2009 American Chemical Society (the scale bar represents 50 nm). (b) Structure of core–shell hierarchical porous carbon materials and corresponding electrode reactions of different discharge platforms [60]. Reprinted with permission from Ref. [60]. Copyright 2009 American Chemical Society. (c) Structure of hierarchical porous carbon to obtain high sulfur accommodation and the cyclic performance curve at high current density [59]. Reprinted with permission from Ref. [59]. Copyright 2014 American Chemical Society.

Core–shell structure and hollow structure: Core–shell nanocomposites can be employed as physical prevention to inhibit the diffusion of polysulfide. On the other hand, polysulfide can be effectively bonded to core–shell structures, which could inhibit the shuttle effect of polysulfide. Meanwhile, the hollow structure provides a large inner cavity, and the shell usually acts as a barrier layer, which could greatly enhance the loading amount of active materials and effectively inhibit the dissolution and diffusion of polysulfides. However, the sulfur species trapped in the inner cavity of the hollow structure are not easily accessible. Therefore, many researchers have tried to optimize the internal cavity to realize the anchoring of polysulfides while ensuring the rapid transfer of the electrolyte, electrons and Li^+ ions toward the active species.

Due to its insulating properties and the shuttle effect of polysulfides, Li_2S exhibits poor utilization of active substances and a short cycle life. Based on these, core–shell $Li_2S@C$ nanocomposites were prepared using plasma sparking and subsequent vulcanization process, through which Li_2S particles could be uniformly coated with a carbon layer of 0.8 nm [61]. It was demonstrated that the carbon coating effectively increases the conductivity of the composite material and effectively reduces the shuttle effect, resulting in superior electrochemical performances (Figure 5a). In addition, a solution evaporation method collaborated with a CVD process was adopted to prepare core–shell $Li_2S@C$

composites (Figure 5b) [62]. The homogeneous amorphous carbon layer with a thickness of about 20 nm was evenly coated on Li_2S , which effectively prevents Li_2S from agglomeration. Compared to the pure Li_2S electrode, the core-shell $\text{Li}_2\text{S}@C$ composite cathode shows high utilization rate of active species and excellent electrochemical performances. In addition, core-shell carbon spheres were prepared via the templating method, which compose of a mesoporous shell, a hollow cavity and a fixed carbon core (Figure 5c) [63]. When used as a carbonaceous sulfur carrier, the hollow cavity can improve the sulfur loading amount and reduce the volume expansion during the charge-discharge process. The mesoporous shell can provide a Li^+ transport channel and inhibit the shuttle effect of polysulfide. In general, this core-shell structure could function as both a physical buffer and a conductive matrix to maximize the potential capacity of active substances and alleviate the intrinsic deficiencies of LSBs.

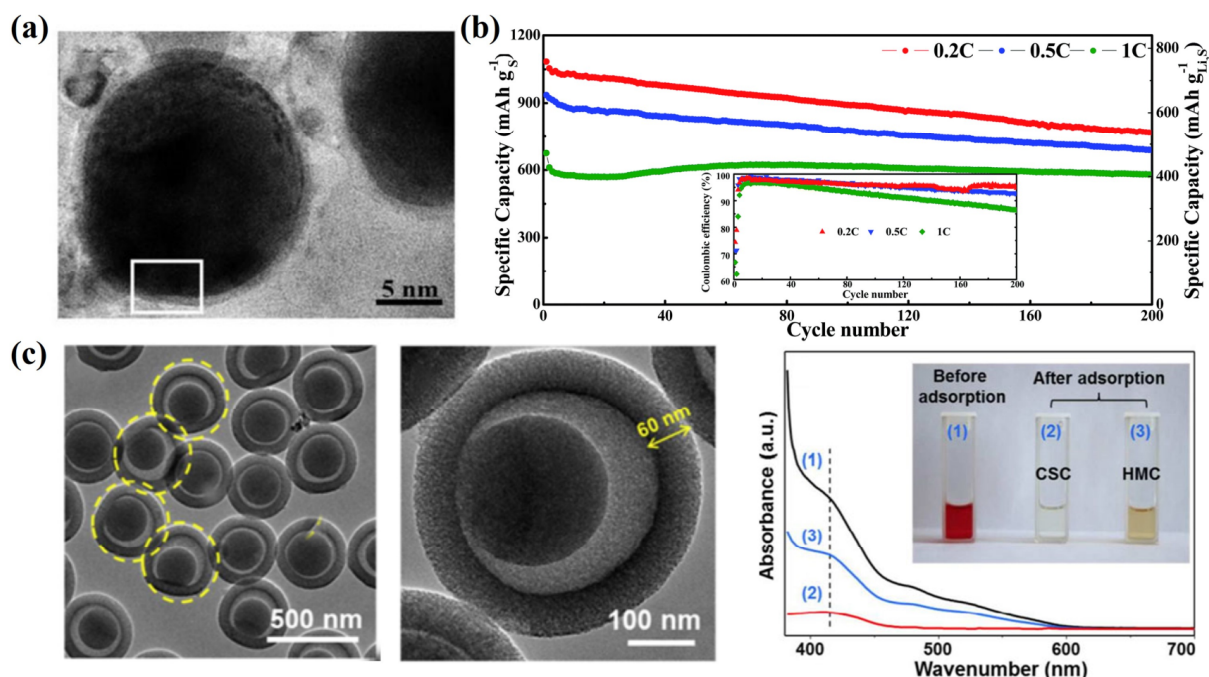


Figure 5. (a) TEM images of the core-shell structure $\text{Li}_2\text{S}@C$ nanocomposites [61]. Reprinted with permission from Ref. [61]. Copyright 2012 Royal Society of Chemistry (the white square highlights the carbon layer on the Li_2S particle). (b) The cyclic performances of the nanocore-shell $\text{Li}_2\text{S}@C$ composites [62]. Reprinted with permission from Ref. [62]. Copyright 2012 Royal Society of Chemistry. (c) TEM images and anchoring ability for polysulfides of hollow yolk-and-shell carbon spheres [63]. Reprinted with permission from Ref. [63]. Copyright 2017 American Chemical Society.

Graphene: Graphene represents a new kind of two-dimensional material with a hexagonal lattice structure composing of sp^2 carbon domains. The π - π conjugated bonding among carbon atoms endows graphene with excellent electrical conductivity. In addition, graphene with a high surface area, high conductivity and stable physical and chemical properties could serve as a potential candidate for LSBs. For example, a simple one-step method was developed to anchor sulfur nanocrystals to 3D cross-linked fibrous graphene (Figure 6a) [64]. When used as the cathode material for Li-sulfur batteries, the porous three-dimensional conductive network and uniformly distributed sulfur nanocrystals achieve rapid electron transport and shorten Li^+ diffusion distance. In addition, the presence of oxygen-containing functional groups enhances the anchoring ability of polysulfide and prevents the dissolution of polysulfide in the electrolyte, which amounts to the high capacity, high-rate performance and long cycle life. Moreover, graphene foam electrodes were proposed and prepared through an effective strategy to obtain flexible Li-sulfur batteries with high energy and power densities as well as long cycle life (Figure 6b) [65].

This research found that graphene foams can provide highly conductive networks, strong mechanical support and enough room for a high sulfur loading amount. In order to further enhance the electrochemical performances, hollow nanographene spheres (GSs) supported by carbon nanotubes (CNTs) were prepared using a room-temperature solubility-processable method (Figure 6c) [66]. Within the unique flexible electrode, the conductive carbon nanotubes could serve as flexible scaffolds and the hollow GSs provide a closed space to accommodate the sulfur species, which could adapt to the volume expansion and inhibit the shuttle and dissolution of polysulfides, leading to rapid electron and ion transport.

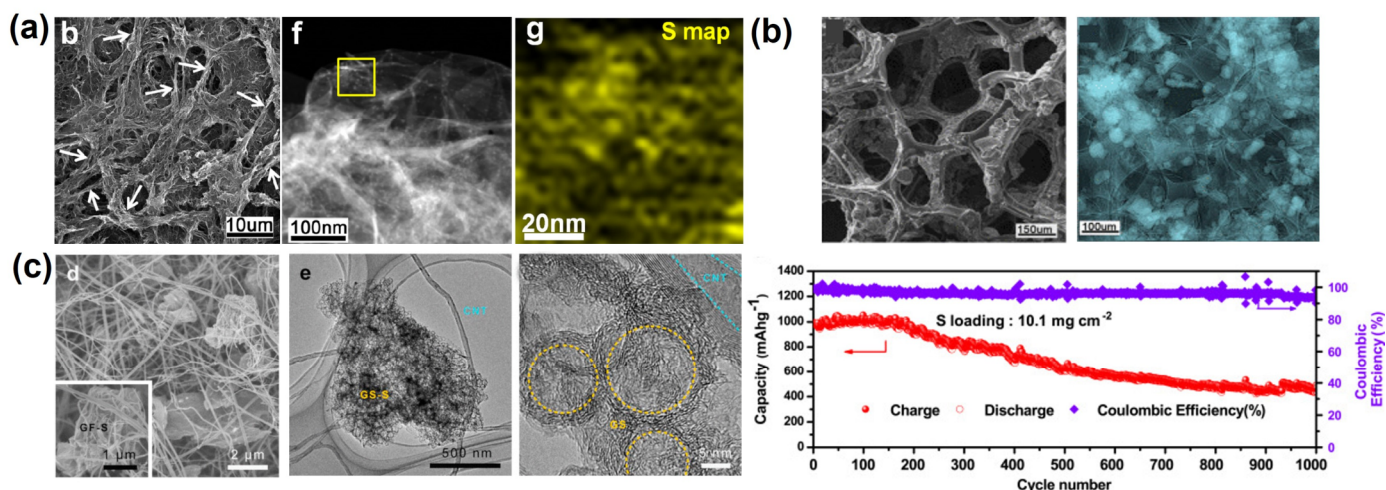


Figure 6. (a) SEM, TEM images and the corresponding S element map of the fibrous graphene/sulfur composites [64]. Reprinted with permission from Ref. [64] (the white arrows represent the fibrous graphene, and the yellow square indicates the sulfur map region of the samples). Copyright 2013 American Chemical Society. (b) The SEM and element map images of the self-supported graphene foam electrode (top), as well as their cycling performances of the corresponding LSB with high S loading density. [65]. Reprinted with permission from Ref. [65]. Copyright 2014 Elsevier Ltd. (c) SEM and TEM images of the carbon nanotube-supported hollow graphene spheres [66]. Reprinted with permission from Ref. [66]. Copyright 2014 Elsevier Ltd (the yellow circles represent the hollow graphene spheres).

3.2. Heteroatom-Doped Carbons for Cathode Materials

Nonmetallic heteroatoms (N, O, S, P, etc.) can be used as anchoring sites for polysulfides. Therefore, in addition to structural design, the introduction of heteroatoms into the conductive carbon matrix is also an effective way to improve the performance of batteries. Due to the electronegativity difference, electron-rich heteroatoms can lead to the surface polarization of the non-polar conductive carbon matrix, which helps to improve the chemical anchoring ability of the carbon matrix to polysulfide. At the same time, heteroatom impurity can introduce defect sites to enhance the catalytic performances of the electrodes so as to enhance the conversion of polysulfides. As shown in Figure 7a, nitrogen-doped mesoporous carbon microspheres permeated by carbon nanotubes as sulfur hosts were prepared through a self-assembly method, which greatly improves the performance of the batteries [67]. Due to the interaction between Li⁺ and N atoms, soluble polysulfide in the electrolyte can be anchored by forming stable Li₂S_x-N chemical bonds, and polysulfide can be confined to the cathode materials, which significantly inhibits the shuttle effect and improves the electrochemical performance of the battery. Unlike conventional insulating adsorbents, nitrogen doping can inhibit the shuttle effect through the chemical interaction between the doping site and polysulfide. At the same time, the high conductivity of the nitrogen-doped carbon materials can directly trigger the conversion of polysulfides at the electrodes. For example, boron is a typical electron-deficient element, which can interact

with electron-rich sulfur and polysulfide to form stable chemical bonds and, thus, can be used to absorb polysulfide and inhibit the shuttle effect. Han et al. prepared a boron-doped porous carbon material as the sulfur carrier [68] (Figure 7b). Compared to the undoped porous carbon, the boron-doped material showed high initial capacity (1300 mA h g^{-1} , 0.25 C), good cyclic stability and superior rate performance. Based on the mechanism study, boron, with a lower electronegativity than carbon, provides positively charged active sites, which could effectively adsorb negatively charged polysulfide.

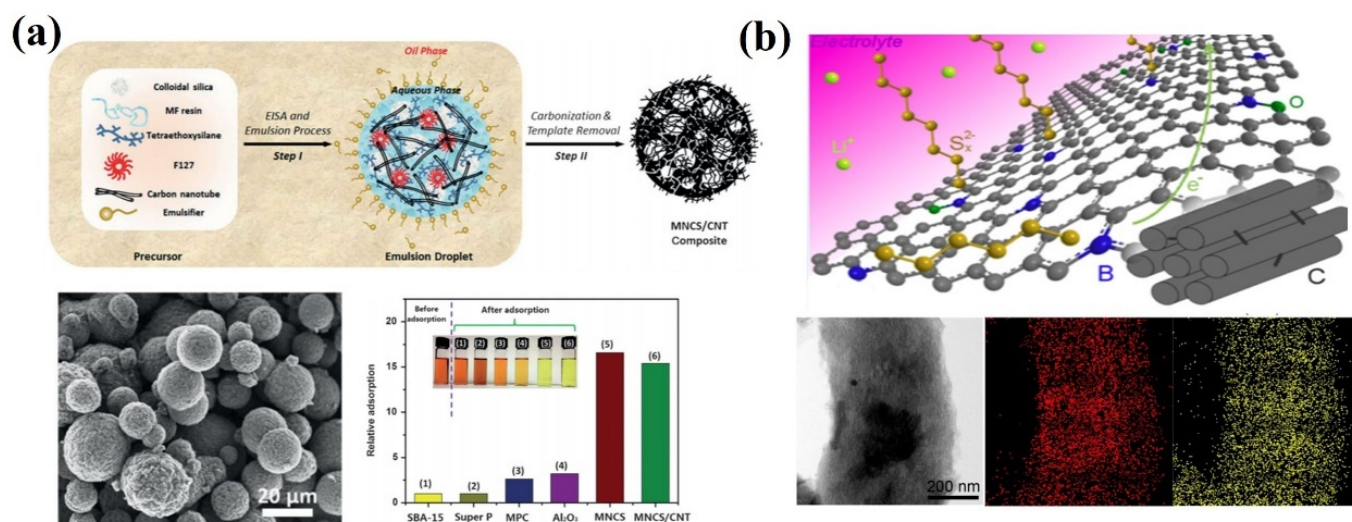


Figure 7. (a) Preparation routes, SEM images and polysulfide anchoring ability of carbon nanotube-penetrated nitrogen-doped mesoporous carbon microspheres [67]. Reprinted with permission from Ref. [67]. Copyright 2015 Wiley-VCH. (b) Mechanism diagram, STEM image and element distribution diagram of boron-doped ordered porous carbon/sulfur electrode material [68]. Reprinted with permission from Ref. [68]. Copyright 2014 American Chemical Society.

Compared to the single doping effect, the co-doping of heteroatoms can effectively combine the advantages of different heteroatoms, which can greatly improve the conductivity of carbon matrix and the adsorption of polysulfide. Diketoxime (DMG) and nickel chloride tetrahydrate ($\text{NiCl}_2 \cdot 4\text{H}_2\text{O}$) were used as precursors for the preparation of nitrogen and oxygen co-doped porous carbon microrods with a large specific surface area and high porosity (Figure 8a) [69]. Based on the density functional theory (DFT) calculation, it is confirmed that the introduction of nitrogen and oxygen heteroatoms can effectively improve the adsorption capacity of the carbon matrix toward polysulfides and greatly inhibit the shuttle effect, which significantly improves the electrochemical performance of LSBs. Graphene oxide nanoribbons were modified by adding boric acid and urea to obtain nitrogen and boron co-doped curved graphene nanoribbons [70]. It was found that the reaction of the boric acid/urea precursor could promote the co-doping process of nitrogen and boron. In addition, the rich N-B motifs could significantly improve the electron conductivity, sulfur dispersion and polysulfide adsorption capacity of the electrodes. Wang et al. developed an effective strategy to improve the electrochemical performance of sulfur electrodes via the preparation of nitrogen/sulfur co-doped graphene matrix for the cathode material of LSBs [71]. In addition to the chemical anchoring of polysulfide by the nitrogen and sulfur defect sites, nitrogen and sulfur atoms with high electronegativity lead to the polarization of adjacent carbon atoms and oxygen-containing functional groups, which could increase the adsorption activity of sulfur and polysulfide. At the same time, the highly developed defects and edges and the porous structures obtained via the chemical activation of graphene not only achieve good dispersion of sulfur, but also act as a polysulfide reservoir to mitigate the shuttle effect. In addition, lithium iron phosphate nanoparticles were adopted as a hard template to prepare nitrogen, oxygen and phosphorus co-doped hollow carbon nanocapsules/graphene composites as the sulfur cathode [72]. The shuttle

effect of polysulfide could be greatly inhibited by the physical and chemical adsorption of the abundant surface polar groups on the composite material.

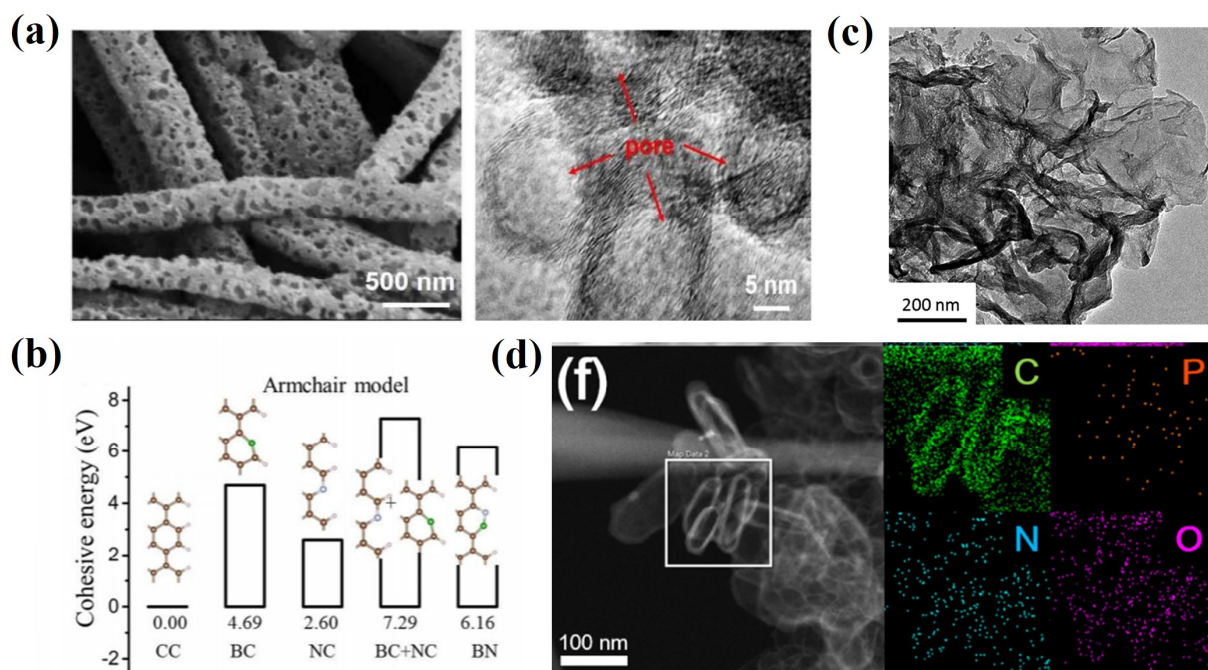


Figure 8. (a) SEM and TEM images of nitrogen–oxygen co-doped porous carbons [69]. Reprinted with permission from Ref. [69]. Copyright 2018 American Chemical Society. (b), The binding energy of polysulfide with different element doping patterns of the N-B co-doped curved graphene nanoribbon [70]. Reprinted with permission from Ref. [70]. Copyright 2012 Royal Society of Chemistry. (c) TEM image of nitrogen–sulfur co-doped porous graphene [71]. Reprinted with permission from Ref. [71]. Copyright 2012 Royal Society of Chemistry. (d) TEM image and element distribution of nitrogen, oxygen and phosphorus co-doped hollow carbon nanocapsules/graphene composites [72]. Reprinted with permission from Ref. [72]. Copyright 2018 American Chemical Society.

4. Biomass-Derived Carbon Materials for LSBs

4.1. Advantages of Biomass-Derived Carbon Materials

Compared to other non-renewable carbon sources, biomass can be used as an abundant and sustainable carbon source to prepare porous carbon materials for energy storage and conversion [73]. So far as we know, a large variety of biomasses have been used as biomass carbon sources to prepare carbon materials as sulfur carriers or functional separators in lithium–sulfur batteries [74]. Compared to other carbon sources, biomass precursors have the following advantages. First of all, after thousands of years of evolution, biomass usually possesses a unique structure and morphology. The inherent hierarchical channel structure obtained after carbonization is conducive to sulfur accommodation and adsorption, which could potentially alleviate the volume expansion of cathodes. Secondly, biomass precursors have diversified compositions. In the process of carbonization, a biomass's inherent heteroatoms could be doped into a carbon matrix, which could enhance the conductivity and the adsorption of polysulfides through the strong chemical interactions. Finally, due to the massive production of biomasses annually from different industries, biomass-derived carbons with a low price could substantially reduce the commercial production cost of LSBs.

4.2. Biomass-Derived Carbons for the Cathode of LSBs

Biomasses, such as agriculture wastes [75–79], forest wastes [80–83], weeds [84–86], food residues [87–100], and so on, have been developed as precursors to prepare high-performance carbons as cathode hosts for LSBs. As shown in Figure 9a, N, O co-doped carbon with a hierarchical porous structure was derived from bagasse, which could serve as

a novel sulfur host for stable LSBs. It was found that the interconnected hierarchical porous structure facilitates the charge transport and alleviates the volume expansion of sulfur during the lithiation process, which finally amounts to highly stable LSBs [75]. In addition, a novel biomass waste, garlic peel, was used as a precursor to prepare carbons through two methods, pre-carbonization and hydrothermal treatment (Figure 9b). Due to the high surface area of carbon, the cathode exhibits high initial specific capacity and cycle retention. These structure advantages could also lead to the intimate contact between sulfur and the conductive carbon matrix, which could physically confine lithium polysulfide intermediates and reduce the shuttle effect [79]. Eucommia leaf residue was employed to prepare carbons with a hierarchical porous structure via the co-auxiliary activation of KCl and CaCl₂ with a low dosage of KOH (Figure 9c). The optimized pore distribution, high specific surface area and nitrogen-containing functional groups could enhance the utilization of sulfur and provide a chemical anchor for polysulfides, which gives rise to the excellent electrochemical performances [82]. Moreover, carbon materials with rational tailored morphology and structures could be obtained from balsa waste (Figure 9d). It was found that the mesopores in such carbon materials exhibit more merits than micro/macropores in improving sulfur utilization and restraining Li₂S_x, which could alleviate the notorious shuttle effect. In addition, the mechanism studies show that the conversion from long-chain polysulfide into solid S₈ and Li₂S could be accelerated by oxygen groups, which finally leads to improved sulfur immobilization and stable energy-storage capacity [83].

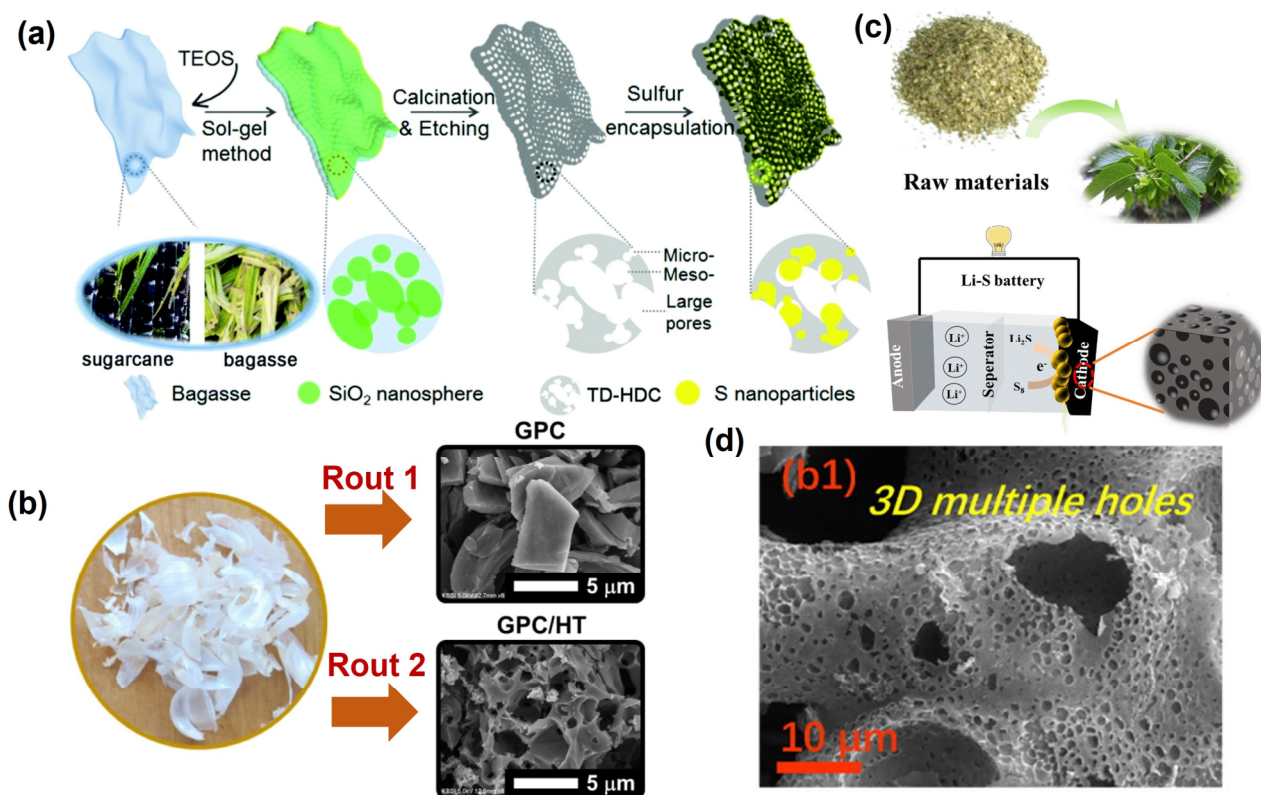


Figure 9. (a) Schematic illustration of the formation process of bagasse-derived carbon/sulfur composite [75]. Reprinted with permission from Ref. [75]. Copyright 2021 Royal Society of Chemistry. (b) Preparation of porous carbons using garlic peels and the SEM images of the carbons derived from different preparation routs [79]. Reprinted with permission from Ref. [79]. Copyright 2021 Elsevier Ltd. (c) The schematic illustration for the synthesis of Eucommia leaf residue-derived hierarchical porous carbon and their application in LSBs [82]. Reprinted with permission from Ref. [82]. Copyright 2023 Elsevier Ltd. (d) The SEM image of oxygen-doped carbon derived from balsa waste [83]. Reprinted with permission from Ref. [83]. Copyright 2021 Elsevier Ltd.

In addition to these biomasses from agriculture, forest wastes and food residues have also been employed as raw materials for the production of carbon as a host for LSBs. As depicted in Figure 10a, nitrogen/sulfur co-doped porous carbons were manufactured from cattail biomass through a one-step hydrothermal method. The stable foam-like porous structure, high specific surface area and N/S atom-doping sites could greatly inhibit the volume expansion of sulfur and the shuttle effect due to the physical confinement and chemical adsorption during the electrochemical process of LSBs [84]. In addition, nitrogen-doped porous carbon was prepared through the carbonization of pomelo peels to serve as a sulfur host material for LSBs (Figure 10b). The N-doping sites and the hierarchical porous architecture render the carbonous material with excellent sulfur confinement property due to the combination of physical and chemical adsorptions. Therefore, the sulfur composite cathodes exhibit ultrahigh initial capacity, high coulombic efficiency and stable sulfur electrochemistry [88]. Moreover, starch was adopted as a precursor to prepare porous carbon materials without using additional physical and chemical activators [97]. In order to avoid damage to the material structure caused by rapid generation and aggregation of water vapor during pyrolysis, the heating rate and airflow velocity during pyrolysis were carefully controlled (Figure 11a). The as-synthesized carbon material possesses the inherent porous structure of starch, which effectively increases the pore volume of the as-obtained carbon material. It was found that the narrow and long microporous channel not only avoids the direct contact between the electrolyte and active substances, but it also immobilizes polysulfide in the porous shell through physical adsorption, which effectively inhibits the shuttle effect of soluble polysulfide. To further optimize the pore structure of carbon products, mesoscale silica spheres with a uniform size were used as hard templates, which endows the as-obtained carbon with ordered structure and uniform pore size (Figure 11b). The abundant mesoporous structure provides enough space for the storage of active substances and alleviates the volume expansion during lithiation, which greatly overcomes the electronic insulation of sulfur and effectively inhibits the migration of polysulfides [98]. Nitrogen and oxygen co-doped porous carbon materials could also be obtained from soybeans [100]. The protein contained in this precursor is converted into different nitrogen-containing components (pyrrole nitrogen, pyridine nitrogen and graphite nitrogen) during pyrolysis, which leads to a higher nitrogen content in these electron donors to improve the overall electron density of the carbon materials and enhances the conductivity of the carbon materials. In addition, nitrogen-doping sites can be employed as electron-donating sites to bind electron-deficient polysulfides with strong chemical bonds, thus enhancing the anchoring ability of the carbon framework to polysulfides (Figure 11c). Based on the traditional Chinese expansion method, rice was employed as a precursor to prepare porous carbons composed of nickel-doped hybrid nanoflakes [99] (Figure 11d). After expansion, the dense starch structure becomes loose due to steam evaporation. It was found that the final carbon with a sheet-like structure provides a stable three-dimensional porous structure, which avoids the structural collapse caused by volume change during the charge and discharge process. The three-dimensional porous structure, as the space for storing active substances, ensures the electrical contact between the active substances and the conductive network. In addition, the stable chemical bond between Ni/NiO and polysulfide effectively alleviates the shuttle effect and ensures a high-capacity retention rate. Meanwhile, the embedded nickel nanoparticles not only significantly increase the electronic conductivity but also provide a shortened ion diffusion channel to accelerate the diffusion process. In order to further highlight the recent developments in biomass-derived carbons adopted as cathodes in LSBs, a systematic comparison table is provided in terms of the preparation method and the electrochemical performances of LSBs (Table S1).

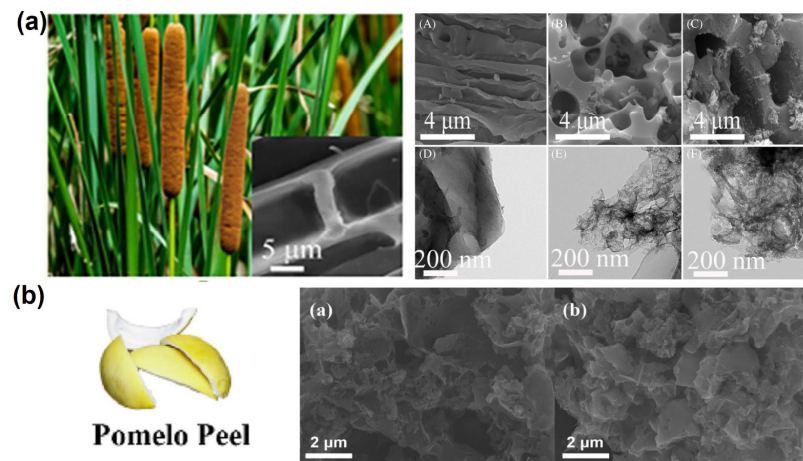


Figure 10. (a) Photograph of the cattail biomass, SEM and TEM images of the cattail derived carbons prepared based on different processes. [84] Reprinted with permission from Ref. [84]. Copyright 2022 John Wiley and Sons. (b) Illustration of the pomelo peels, and the SEM images of the as-synthesized carbons before (left) and after (right) sulfur loading [88]. Reprinted with permission from Ref. [88]. Copyright 2020 Elsevier Ltd.

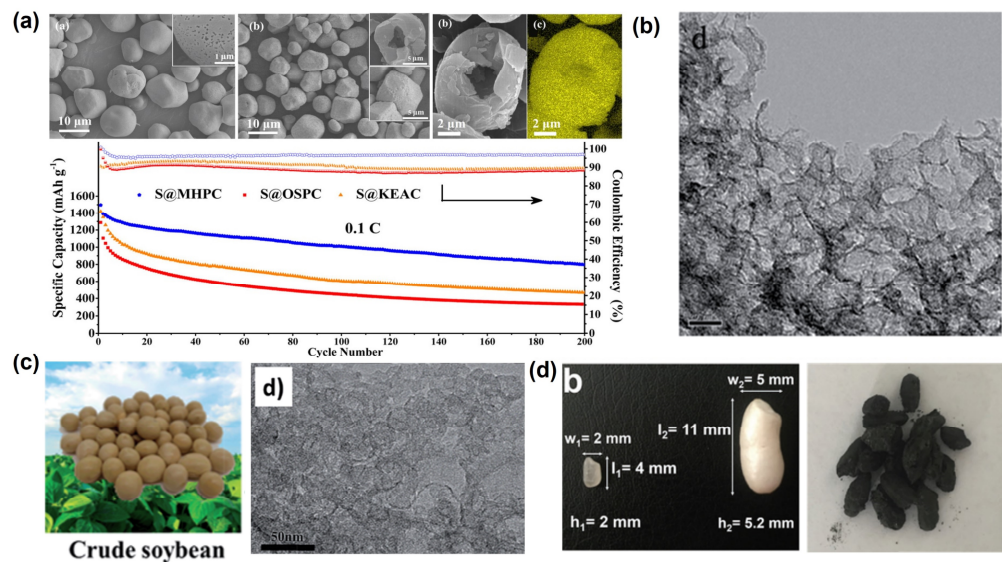


Figure 11. (a) Morphology of the hollow microporous carbon spheres prepared from starch via a multi-step pyrolysis method and their cycling performance at 0.1 C [97]. Reprinted with permission from Ref. [97]. Copyright 2017 American Chemical Society. (b) The TEM image of nitrogen–sulfur co-doped carbon materials prepared from soluble starch via a template method [98]. Reprinted with permission from Ref. [98]. Copyright 2012 Royal Society of Chemistry (The scale bar represents 20 nm). (c) Photograph of the crude soybean biomass and the TEM image of the nitrogen–oxygen co-doped porous carbon materials prepared by using soybean as a precursor [100]. Reprinted with permission from Ref. [100]. Copyright 2016 Royal Society of Chemistry. (d) The photograph of the rice before and after expansion treatment, as well as the photograph of the nickel-doped hybrid carbon prepared based on the expansion technology and calcination [99]. Reprinted with permission from Ref. [99]. Copyright 2017 WILEY-VCH.

4.3. Biomass-Derived Carbons for the Interlayer of LSBs

In order to enhance the performance of LSBs, free-standing or deposited interlayers, which could effectively prohibit the shuttle effect of polysulfides, have been designed and introduced between the electrodes without affecting the integrity of LSBs. So far as we know, many types of biomass-derived carbons have been adopted to modify the pristine

separator or construct a free-standing interlayer between the electrodes of LSBs [101–104]. As depicted in Figure 12a, N, O co-doped carbons with a hierarchical porous structure, a high specific surface area, and good electrical conductivity were synthesized from chlorella biomass through a chemical activation process. As they are deposited on the polypropylene separator as an interlayer in LIBs, these carbons can improve the electrolyte wettability and Li^+ diffusion. In addition, N, O heteroatoms and the porous structure exhibit strong chemical adsorption and provide physical barriers confining lithium polysulfides, which result in enhanced cycling stability and rate performance. As shown in Figure 12b, Ginkgo Folium was employed as a biomass to synthesize carbon materials to decorate the separator of LSBs. Thanks to the three-dimensional interconnected porous structures and the defective graphite structure, the interlayer effectively inhibits the shuttle effect and boosts the electrochemical properties of the LSBs. In addition, rotten egg albumen-derived carbon was also fabricated via freeze drying and carbonization (Figure 12c). As modified on the separator, the layered carbon materials with high conductivity and the rich nitrogen-doped sites could enhance both lithium ion and electrical conductivity, and improve polysulfide adsorption, which substantially inhibits the shuttle effect of polysulfides and enhances the electrochemical performance of LSBs.

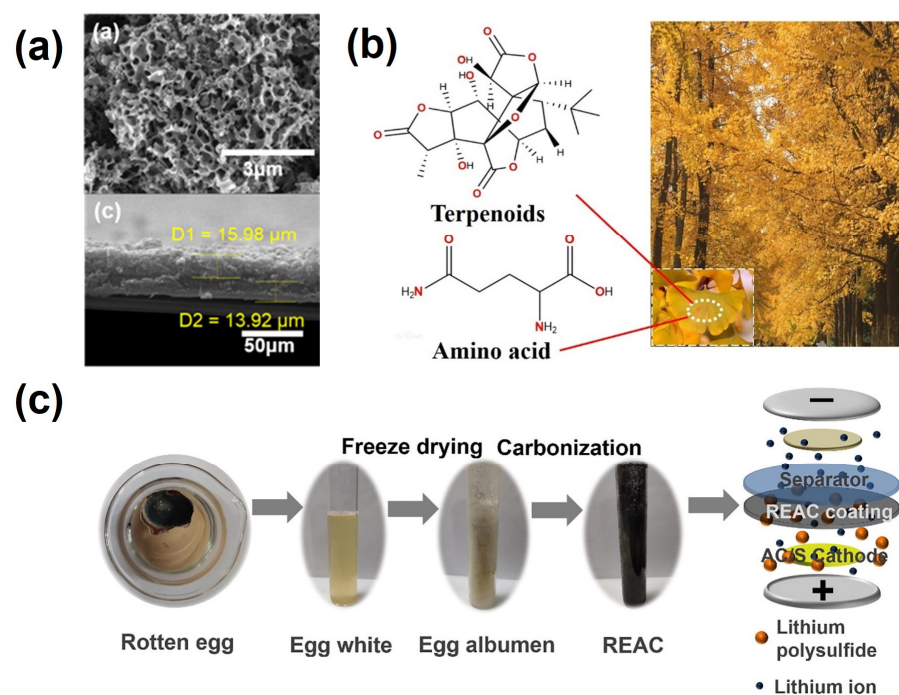


Figure 12. (a) SEM images of the top and cross-section morphology of chlorella-derived carbon-coated separator [101]. Reprinted with permission from Ref. [101]. Copyright 2020 Elsevier Inc. (b) Chemicals contained in the Ginkgo Folium biomass [103]. Reprinted with permission from Ref. [103]. Copyright 2022 Elsevier Inc. (c) Synthesis process of rotten egg-derived carbon-modified separator [104]. Reprinted with permission from Ref. [104]. Copyright 2021 Elsevier Inc.

As shown in Figure 13a, discarded crab shells were employed as a precursor to yield functional carbon materials through potassium hydroxide-assisted pyrolysis [105]. Due to the intrinsic rich keratin content contained in the crab shells, nitrogen doping could be easily introduced during pyrolysis. As deposited on the membrane surface of the separator, the surface wettability is greatly improved and strong chemisorption of polysulfides is formed, which could effectively enhance the electrolyte permeability, the transportation of lithium ions and the adsorption of the modified separator. As depicted in Figure 13b, bamboo chopsticks were used to prepare carbon fibers as an interlayer for LIBs with excellent electrochemical performances [106]. When used as an interlayer for LSBs, soluble polysulfides can be effectively adsorbed in the bamboo carbon fiber sandwich membrane,

and the shuttle effect is substantially suppressed. At the same time, the cross-linked three-dimensional conductive framework constructed by the fiber structure also provides an interworking conductive network, which promotes both the electronic transport and the diffusion rate of lithium ions. In addition, sulfur-doped microporous carbon materials could be prepared from loofah pulp biomass. The as-prepared self-supporting porous carbons could effectively prevent the diffusion of polysulfides to improve the electrochemical performance of LSBs [107]. The mechanism studies indicated that the rich microporous structure and sulfur-doping sites could be used as both physical and chemical adsorption sites, which could effectively adsorb polysulfides in the conductive framework and avoid the irreversible loss of active substances, leading to high sulfur utilization and high cycle stability. Recent research progresses regarding biomass-derived carbons adopted as an interlayer in LSBs are summarized in Table S2.

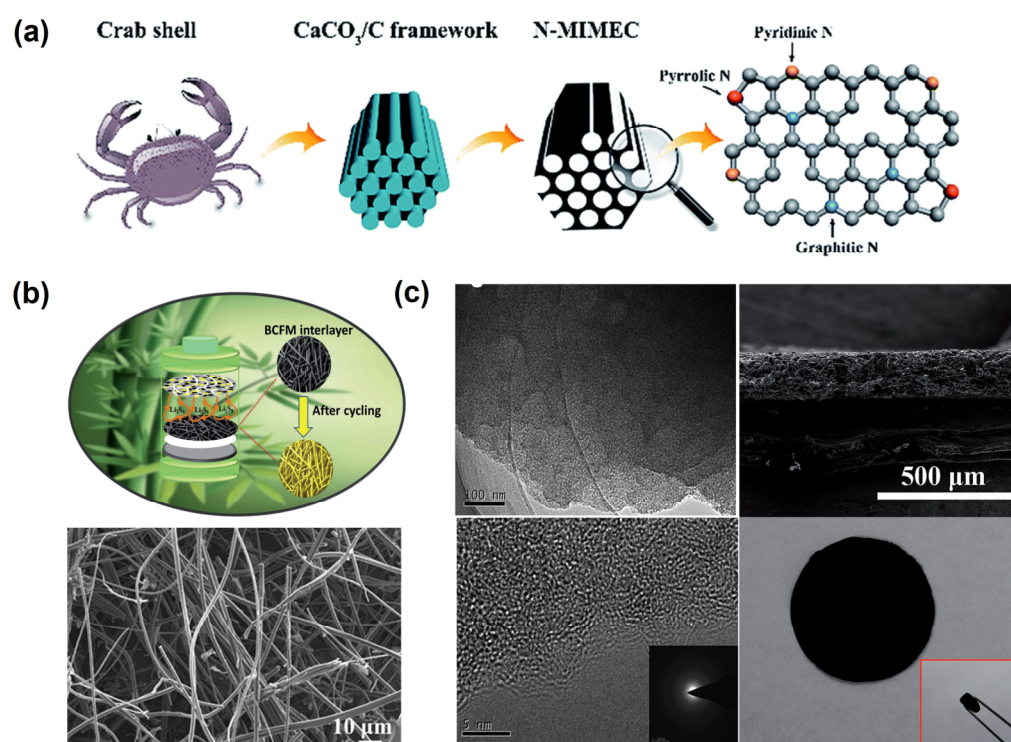


Figure 13. (a) Preparation route and the N doping sites of the hierarchical porous carbon materials prepared from crab shells [105]. Reprinted with permission from Ref. [105]. Copyright 2018 Royal Society of Chemistry. (b) Fabrication scheme and SEM image of hollow carbon fiber networks prepared from discarded bamboo chopsticks [106]. Reprinted with permission from Ref. [106]. Copyright 2012 Royal Society of Chemistry. (c) TEM, SEM images and the photograph of the self-supporting sulfur-doped porous carbon sandwich membrane prepared from loofah pulp [107]. Reprinted with permission from Ref. [107]. Copyright 2012 Royal Society of Chemistry.

4.4. Modified Biomass-Derived Carbons for LSBs

The main advantages of biomasses rely on their intrinsic heteroatoms and porous structure, which could endow the as-obtained carbonous materials with a high surface area, a hierarchical porous structure and heteroatom-doping sites. However, these merits highly depend on the inherent qualities of the biomass used, which is not favorable for further property enhancement of carbon materials. Therefore, many schemes have been developed to modify the biomass used prior to or after the carbonization process [108]. As shown in Figure 14a, in order to introduce P doping sites on the carbon materials, H_3PO_4 was added in cotton stalk biowaste, which could both enhance the surface area and introduce hierarchical pores. The P doping sites in the carbon networks not only provide more active sites but also improve the electrical conductivity, which finally results in excellent

electrochemical performances [109]. In addition, CoO nanoparticles were decorated on hierarchical porous carbon by mixing a natural nori and Co precursor prior to the carbonization process. It was found that the carbon substrate could well accommodate CoO nanoparticles, which could enhance the adsorption immobilization of lithium polysulfides and facilitate their redox conversion. Therefore, the composite cathode possesses a high discharge capacity, excellent rate performance and cycling stability [110–116]. As shown in Figure 14b, rice straw was developed to fabricate conductive biochar and then decorated with highly dispersed CoO nanoparticles via a microwave-assisted method. The high LSB performances are derived from the excellent conductive framework of the biochar and the excellent adsorption capability of CoO nanoparticles, which greatly alleviate the shuttle effect as well as the conversion kinetics between the polysulfides [115].

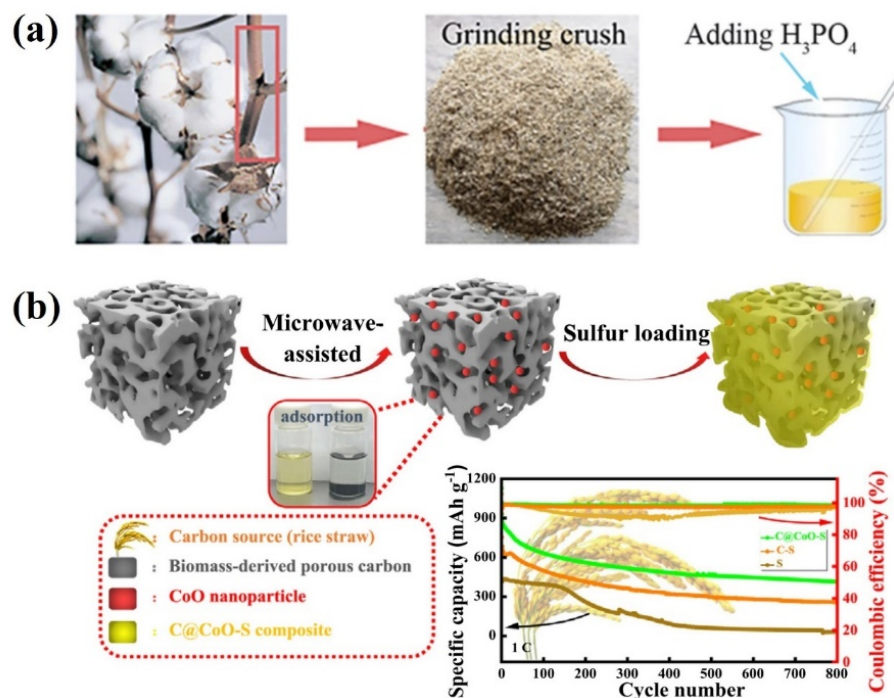


Figure 14. (a) Schematic illustration of the preparation procedure of P-doped carbon materials from cotton stalk biowaste [108]. Reprinted with permission from Ref. [108]. Copyright 2022 American Chemical Society. (b) Highly dispersed CoO nanoparticles are formed in the inner channels of biochar via microwave-assisted treatment. [115] Reprinted with permission from Ref. [115]. Copyright 2023 Elsevier Inc.

Based on a similar concept, activated cotton textile was adopted as a scaffold to load Fe/Fe₃C-encapsulated multiwalled carbon nanotubes via a strategy combining vapor–liquid–solid and solid–liquid–solid processes (Figure 15a). The as-prepared composite was employed as a free-standing interlayer for LIBs, which leads to high cycling stability, ultralow capacity decay rate and remarkable specific capacity due to the enhanced electrode stability and suppressed shuttle effect of polysulfides [117]. In addition, phytoremediation residue-derived carbons were used as a host for LSBs. After the phosphorous acid-assisted pyrolysis of oilseed rape stems from phytoremediation, the as-yield carbon materials with a porous structure and abundant N, P, O doping sites could effectively enhance the sulfur loading amount and polysulfide adsorption, which lead to excellent electrochemical performances. This research not only proposed a promising approach for the safe disposal of phytoremediation residues but also high-performance cathode materials for LSBs [118]. As depicted in Figure 15b, carbon materials were prepared from brewing waste without any activation process. These carbons demonstrate high surface area and interconnected micro- and mesoporous distributions, which raises the capacity values and cyclability of

LSBs. This work demonstrated a promising and sustainable way to yield porous carbons while adopting a simple process without activation process.

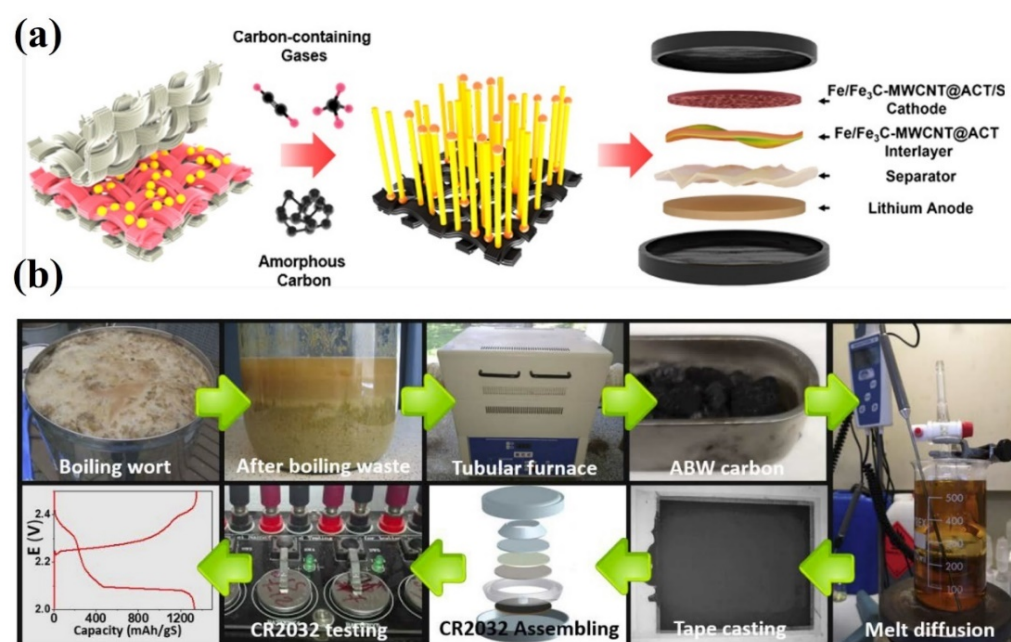


Figure 15. (a) Schematic of cotton-derived Fe/Fe₃C-encapsulated multiwalled carbon nanotubes' interlayer and their application in LSBs [117]. Reprinted with permission from Ref. [117]. Copyright 2022 American Chemical Society. (b) Scheme of cathode fabrication from beer production waste for LSBs [119]. Reprinted with permission from Ref. [119]. Copyright 2020 Wiley-VCH.

5. Conclusions and Outlook

Due to their low cost, abundance in resources and environmentally friendly qualities, biomasses generated from different scenarios have been employed to prepare carbon matrices as host or interlayer materials for LSBs. Many case works have proven that a hierarchical porous structure and heteroatom-doping sites inherited from the tissue of the biomass used are the main advantages to enhance sulfur utilization, prohibit the shuttle effect of polysulfides, and accelerate the sluggish redox conversion of soluble intermediates. Although remarkable research works have been devoted to the rational design and preparation of biomass-derived carbons, several bottlenecks still remain and require further investigation. The first challenge is that the activation of carbons usually needs corrosive or even poisonous chemical reagents, such as NaOH, KOH, and ZnCl₂, which hinders the commercialization of biomass derived carbons. Although previous works have been devoted to preparing biomass-derived carbons without further activation or purification [119,120], more efforts should be devoted to developing green and low-toxic pore regulation strategies. Secondly, many of the reported sources of biomasses are rather limited in quantity or unstable in quality, which usually exhibit unexpected variation in their structure and composition, resulting in adverse impacts on the standard production of such carbon materials. The third obstacle is the inadequate test equipment used to characterize the structure evolution of biomass-derived carbons during their charge and discharge processes, which makes the underlying work mechanism of these carbons in LSBs difficult to be revealed. The final problem is the relative low loading amount of active species on the cathode of LSBs. It has been reported that the S loading amount could be enhanced to above 2 mg cm⁻² [121,122] or even 5 mg cm⁻² [123–125]. However, there is still a distance to meet the requirement for real application scenarios.

Based on these aforementioned challenges, future efforts in the design and production of biomass-derived carbons should be focused on the following aspects. First of all, low-cost, low-energy-consumption and ecofriendly strategies should be further explored for

the massive production of biomass-derived carbons. For example, mild activation methods should be developed to reduce hazardous emission, potential safety concerns and corrosion on the equipment used. In addition, more fundamental understanding should be realized regarding the activation processes, such as the doping process of heteroatoms, the surface modification of different functional groups, and the regulation of porous structures and their conductivities. Further exploration of the formation mechanism of biomass-derived carbons could provide more specific instruction on the potential mass production of these high-performance carbons.

Secondly, in order to achieve the commercialization of biomass-derived carbons for LSBs, a standard production process should be established based on biomasses with high yield and abundant resources. For example, the composition and structure of biomasses vary dramatically as they are harvested in different seasons or at different locations. Even with the same biomass, different preparation methods usually lead to different structural qualities of carbons. Therefore, in order to provide stable and high-performance carbons for LSBs, many standards should not only be established for the collection and pretreatment of biomasses but also for the pyrolysis process and posttreatment.

Thirdly, advanced equipment composed of microscopy, spectroscopy and X-ray absorption should be designed and assembled to observe in situ the structure, composition and morphology evolution of biomass-derived carbons during the operation of LSBs, which could help to accurately select the appropriate carbons to attain a high-performance cathode or interlayer for LSBs. In particular, the characterization of the electrolyte's decomposition and conversion on the surface of the carbon electrode could provide straightforward evidence to enhance the coulombic efficiency, rate performance and cycling stability of LSBs.

Finally, the production of carbons from biomasses not only reduce the environmental burden from biomasses or biowastes generated in different industries but also pave an ecofriendly way for backing up the utilization of renewable energy with high-performance energy storage devices. However, an unneglectable fact that should not be omitted is that the activation, pyrolysis and purification processes during the production generate a large volume of liquid and gaseous effluents, and require high energy and chemical reagent consumptions, which will again lead to a huge environmental burden. Therefore, systematic environmental and economic sustainability studies should be devoted to the green and standardized mass production of biomass-derived carbons, which could provide more opportunities for the final commercialization of biomass carbon-derived LSBs.

Supplementary Materials: The following supporting information can be downloaded at <https://www.mdpi.com/article/10.3390/nano13111768/s1>. Table S1: Biomass-derived carbons for the cathode of LSBs; Table S2: Biomass-derived carbons for the interlayer of LSBs.

Author Contributions: C.M.: Data curation; Formal analysis; Writing-original draft; M.Z.: Conceptualization; Data curation; Validation; Writing-original draft. Y.D.: Data curation; Formal analysis. Y.X.: Formal analysis; Supervision; Writing-review & editing. H.W.: Formal analysis; Validation. P.L.: Data curation; Formal analysis. D.W.: Conceptualization; Funding acquisition; Supervision; Writing-review & editing. All authors have read and agreed to the published version of the manuscript.

Funding: This study was funded by the Key Science and Technology Project of Henan Province (21A430022), the Soft Science Research Program of Henan Province (212400410310), the Outstanding Youth Science Foundation of HTU (2021JQ03), and the Natural Science Foundation of Henan Province (212300410009).

Informed Consent Statement: Informed consent was obtained from all subjects involved in the study.

Data Availability Statement: The data is available upon request.

Conflicts of Interest: The authors declare no conflict of interest.

References

1. Zhang, W.C.; Lu, J.; Guo, Z.P. Approaching high-performance potassium-ion batteries via advanced design strategies and engineering. *Sci. Adv.* **2019**, *5*, eaav7412. [[CrossRef](#)] [[PubMed](#)]
2. Peng, H.J.; Huang, J.Q.; Cheng, X.B.; Zhang, Q. Review on High-Loading and High-Energy Lithium-Sulfur Batteries. *Adv. Energy Mater.* **2017**, *24*, 1700260. [[CrossRef](#)]
3. Zhang, W.C.; Lu, J.; Guo, Z.P. Challenges and future perspectives on sodium and potassium ion batteries for grid-scale energy storage. *Mater. Today* **2021**, *50*, 400–417. [[CrossRef](#)]
4. Zhang, F.L.; Zhang, W.C.; David, W.; Guo, Z.P. Recent Progress and Future Advances on Aqueous Monovalent-Ion Batteries towards Safe and High-Power Energy Storage. *Adv. Mater.* **2022**, *34*, 2107965. [[CrossRef](#)] [[PubMed](#)]
5. Chen, L.F.; Feng, Y.; Liang, H.W.; Wu, Z.Y.; Yu, S.H. Macroscopic-Scale Three-Dimensional Carbon Nanofiber Architectures for Electrochemical Energy Storage Devices. *Adv. Energy Mater.* **2017**, *7*, 1700826. [[CrossRef](#)]
6. Li, Y.; Wu, F.; Li, Y.; Liu, M.Q.; Feng, X.; Bai, Y.; Wu, C. Ether-based electrolytes for sodium ion batteries. *Chem. Soc. Rev.* **2022**, *51*, 4484–4536. [[CrossRef](#)]
7. Sen, X.; Lin, G.; Zhao, N.H. Smaller Sulfur Molecules Promise Better Lithium—Sulfur Batteries. *J. Am. Chem. Soc.* **2012**, *134*, 18510–18513. [[CrossRef](#)]
8. Zhang, J.; Huang, H.; Bae, J.; Chung, S.H.; Zhang, W.K.; Manthiram, A.; Yu, G.H. Nanostructured Host Materials for Trapping Sulfur in Rechargeable Li-S Batteries: Structure Design and Interfacial Chemistry. *Small Methods* **2018**, *2*, 1700279. [[CrossRef](#)]
9. Yang, D.X.; Ren, H.Y.; Wu, D.P.; Zhang, W.C.; Lou, X.D.; Wang, D.Q.; Cao, K.; Gao, Z.Y.; Xu, F.; Jiang, K. Bi-functional nitrogen-doped carbon protective layer on three-dimensional RGO/SnO₂ composites with enhanced electron transport and structural stability for high-performance lithium-ion batteries. *J. Colloid Interface Sci.* **2019**, *542*, 81–90. [[CrossRef](#)]
10. Wu, D.P.; Wang, Y.X.; Wang, F.J.; Wang, H.J.; An, Y.P.; Gao, Z.Y.; Xu, F.; Jiang, K. Oxygen-incorporated few-layer MoS₂ vertically aligned on three-dimensional graphene matrix for enhanced catalytic performances in quantum dot sensitized solar cells. *Carbon* **2017**, *123*, 756–766. [[CrossRef](#)]
11. Wang, L.; Jia, F.; Wu, D.P.; Wei, Q.X.; Liang, Y.; Hu, Y.S.; Li, R.F.; Yu, G.H.; Yuan, Q.P.; Wang, J.S. In-situ growth of graphene on carbon fibers for enhanced cell immobilization and xylitol fermentation. *Appl. Surf. Sci.* **2020**, *527*, 146793. [[CrossRef](#)]
12. Chen, J.L.; Wu, D.P.; Wang, H.J.; Wang, F.J.; Wang, Y.X.; Gao, Z.Y.; Xu, F.; Jiang, K. In-situ synthesis of molybdenum sulfide/reduced graphene oxide porous film as robust counter electrode for dye-sensitized solar cells. *J. Colloid Interface Sci.* **2018**, *524*, 475–482. [[CrossRef](#)] [[PubMed](#)]
13. Zou, X.X.; Wu, D.P.; Mu, Y.F.; Xing, L.Y.; Zhang, W.C.; Gao, Z.Y.; Xu, F.; Jiang, K. Boron and nitrogen Co-doped holey graphene aerogels with rich B-N motifs for flexible supercapacitors. *Carbon* **2020**, *159*, 94–101. [[CrossRef](#)]
14. Li, R.G.; Wu, D.P.; Song, J.K.; He, Y.C.; Zhu, W.Y.; Wang, X.P.; Wang, L.X.; Dube, N.M.; Jiang, K. In situ generation of reduced graphene oxide on 3D Cu-Ni foam as high-performance electrodes for capacitive deionization. *Desalination* **2022**, *540*, 115990. [[CrossRef](#)]
15. Tabani, H.; Khodaei, K.; Moghaddam, A.Z. Introduction of graphene-periodic mesoporous silica as a new sorbent for removal: Experiment and simulation. *Chem. Intermed.* **2019**, *45*, 1795–1813. [[CrossRef](#)]
16. Wang, L.; Yin, Y.L.; Zhang, S.B.; Wu, D.P.; Lv, Y.Y.; Hu, Y.S.; Wei, Q.X.; Yuan, Q.P.; Wang, J.S. A rapid microwave-assisted phosphoric-acid treatment on carbon fiber surface for enhanced cell immobilization in xylitol fermentation. *Colloids Surf. B* **2019**, *175*, 697–702. [[CrossRef](#)]
17. Wang, L.; Shen, Y.; Zhang, Y.X.; Wei, Q.X.; Liang, Y.; Tian, H.L.; Wu, D.P.; Yuan, X.Q.; Yuan, Q.P.; Wang, J.S. A novel surface treatment of carbon fiber with Fenton reagent oxidation for improved cells immobilization and xylitol fermentation. *Microporous Mesoporous Mater.* **2021**, *325*, 111318. [[CrossRef](#)]
18. Wang, L.; Liu, N.; Guo, Z.; Wu, D.P.; Chen, W.W.; Chang, Z.; Yuan, Q.P.; Hui, M.; Wang, J.S. Nitric Acid-Treated Carbon Fibers with Enhanced Hydrophilicity for *Candida tropicalis* Immobilization in Xylitol Fermentation. *Materials* **2016**, *9*, 206. [[CrossRef](#)]
19. Wang, R.; Wang, H.J.; Zhou, Y.; Gao, Z.Y.; Han, Y.; Jiang, K.; Zhang, W.C.; Wu, D.P. Green synthesis of N-doped porous carbon/carbon dot composites as metal-free catalytic electrode materials for iodide-mediated quasi-solid flexible supercapacitors. *Inorg. Chem. Front.* **2022**, *9*, 2530–2543. [[CrossRef](#)]
20. Ma, Z.J.; Wu, D.P.; Han, X.Y.; Wang, H.J.; Zhang, L.M.; Gao, Z.Y.; Xu, F.; Jiang, K. Ultrasonic assisted synthesis of Zn-Ni bi-metal MOFs for interconnected Ni-N-C materials with enhanced electrochemical reduction of CO₂. *J. CO₂ Util.* **2019**, *32*, 251–258. [[CrossRef](#)]
21. Ma, Z.J.; Zhang, X.L.; Wu, D.P.; Han, X.X.; Zhang, L.M.; Wang, H.J.; Xu, F.; Gao, Z.Y.; Jiang, K. Ni and nitrogen-codoped ultrathin carbon nanosheets with strong bonding sites for efficient CO₂ electrochemical reduction. *J. Colloid Interface Sci.* **2020**, *570*, 31–40. [[CrossRef](#)] [[PubMed](#)]
22. Li, H.H.; Wang, Y.X.; Chen, H.Q.; Niu, B.X.; Zhang, W.C.; Wu, D.P. Synergistic mediation of polysulfide immobilization and conversion by a catalytic and dual-adsorptive system for high performance lithium-sulfur batteries. *Chem. Eng. J.* **2021**, *406*, 126802. [[CrossRef](#)]
23. Zhang, M.M.; Huang, K.X.; Ding, Y.; Wang, X.Y.; Gao, Y.L.; Li, P.F.; Zhou, Y.; Gao, Z.; Zhang, Y.; Wu, D.P. N, S Co-Doped Carbons Derived from *Enteromorpha prolifera* by a Molten Salt Approach: Antibiotics Removal Performance and Techno-Economic Analysis. *Nanomaterials* **2022**, *12*, 4289. [[CrossRef](#)] [[PubMed](#)]

24. Wang, C.J.; Wu, D.P.; Wang, H.J.; Gao, Z.Y.; Xu, F.; Jiang, K. Nitrogen-doped two-dimensional porous carbon sheets derived from clover biomass for high performance supercapacitors. *J. Power Sources* **2017**, *363*, 375–383. [[CrossRef](#)]
25. Chen, C.; Han, H.J.; Liu, X.P.; Chen, Y.; Wu, D.P.; Gao, Z.Y.; Gao, S.Y.; Jiang, K. Nitrogen, phosphorus, sulfur tri-doped porous carbon derived from covalent polymer with versatile performances in supercapacitor, oxygen reduction reaction and electro-fenton degradation. *Microporous Mesoporous Mater.* **2021**, *325*, 111335. [[CrossRef](#)]
26. Wang, C.J.; Wu, D.P.; Wang, H.J.; Gao, Z.Y.; Xu, F.; Jiang, K. Biomass derived nitrogen-doped hierarchical porous carbon sheets for supercapacitors with high performance. *J. Colloid Interface Sci.* **2018**, *523*, 133–143. [[CrossRef](#)]
27. Wu, D.P.; Chen, J.L.; Zhang, W.C.; Liu, W.D.; Li, J.Z.; Cao, K.; Gao, Z.Y.; Xu, F.; Jiang, K. Sealed pre-carbonization to regulate the porosity and heteroatom sites of biomass derived carbons for lithium-sulfur batteries. *J. Colloid Interface Sci.* **2020**, *579*, 667–679. [[CrossRef](#)]
28. Wang, C.J.; Wu, D.P.; Wang, H.J.; Gao, Z.Y.; Xu, F.; Jiang, K. A green and scalable route to yield porous carbon sheets from biomass for supercapacitors with high capacity. *J. Mater. Chem. A* **2018**, *6*, 1244–1254. [[CrossRef](#)]
29. Chen, C.; Tian, M.; Han, H.J.; Wu, D.P.; Chen, Y.; Gao, Z.Y.; Gao, S.Y.; Jiang, K. N, P-dual doped carbonaceous catalysts derived from bifunctional-salt activation for effective electro-Fenton degradation on waterborne organic pollutions. *Electrochim. Acta* **2021**, *389*, 138732. [[CrossRef](#)]
30. Bai, X.G.; Ying, L.Y.; Liu, N.; Ma, N.N.; Huang, K.X.; Wu, D.P.; Yin, M.M.; Jiang, K. Humulus scandens-Derived Biochars for the Effective Removal of Heavy Metal Ions: Isotherm/Kinetic Study, Column Adsorption and Mechanism Investigation. *Nanomaterials* **2021**, *11*, 3255. [[CrossRef](#)]
31. Yin, M.M.; Bai, X.G.; Wu, D.P.; Li, F.B.; Jiang, K.; Ma, N.N.; Chen, Z.H.; Zhang, X.; Fang, L.P. Sulfur-functional group tuning on biochar through sodium thiosulfate modified molten salt process for efficient heavy metal adsorption. *Chem. Eng. J.* **2022**, *433*, 134441. [[CrossRef](#)]
32. Bai, X.G.; Zhang, M.M.; Niu, B.X.; Zhang, W.L.; Wang, X.P.; Wang, J.S.; Wu, D.P.; Wang, L.; Jiang, K. Rotten sugarcane bagasse derived biochars with rich mineral residues for effective Pb (II) removal in wastewater and the tech-economic analysis. *J. Taiwan Inst. Chem. Eng.* **2022**, *132*, 104231. [[CrossRef](#)]
33. Ragauskas, A.J.; Williams, C.K.; Davison, B.H.; Britovsek, G.; Cairney, J.; Eckert, C.A.; Frederick, W.J., Jr.; Hallett, J.P.; Leak, D.J.; Liotta, C.L.; et al. The path forward for biofuels and biomaterials. *Science* **2006**, *311*, 484–489. [[CrossRef](#)] [[PubMed](#)]
34. Jain, A.; Balasubramanian, R.; Srinivasan, M.P. Hydrothermal conversion of biomass waste to activated carbon with high porosity: A review. *Chem. Eng. J.* **2016**, *283*, 789–805. [[CrossRef](#)]
35. Wang, J.; Kaskel, S. KOH activation of carbon-based materials for energy storage. *J. Mater. Chem.* **2012**, *22*, 23710. [[CrossRef](#)]
36. Keiluweit, M.; Nico, P.S.; Johnson, M.G.; Kleber, M. Dynamic molecular structure of plant biomass-derived black carbon (biochar). *Environ. Sci. Technol.* **2010**, *44*, 1247–1253. [[CrossRef](#)]
37. Long, C.; Chen, X.; Jiang, L.; Zhi, L.; Fan, Z. Porous layer-stacking carbon derived from in-built template in biomass for high volumetric performance supercapacitors. *Nano Energy* **2015**, *12*, 141–151. [[CrossRef](#)]
38. Gao, S.; Li, X.; Li, L.; Wei, X. A versatile biomass derived carbon material for oxygen reduction reaction, supercapacitors and oil/water separation. *Nano Energy* **2017**, *33*, 334–342. [[CrossRef](#)]
39. Hall, P.J.; Mirzaeian, M.; Fletcher, S.I.; Sillars, F.B.; Rennie, A.J.R.; Shitta-Bey, G.O.; Wilson, G.; Crudenb, A.; Carterb, R. Energy storage in electrochemical capacitors: Designing functional materials to improve performance. *Energy Environ. Sci.* **2010**, *3*, 1238. [[CrossRef](#)]
40. Hou, J.; Cao, C.; Idrees, F.; Ma, X. Hierarchical porous nitrogen-doped carbon nanosheets derived from silk for ultrahigh-capacity battery anodes and supercapacitors. *ACS Nano* **2015**, *9*, 2556–2564. [[CrossRef](#)]
41. Niu, J.; Shao, R.; Liang, J.; Dou, M.; Li, Z.; Huang, Y.; Wang, F. Biomass-derived mesopore-dominant porous carbons with large specific surface area and high defect density as high performance electrode materials for Li-ion batteries and supercapacitors. *Nano Energy* **2017**, *36*, 322–330. [[CrossRef](#)]
42. Gu, X.; Wang, Y.; Lai, C.; Qiu, J.; Li, S.; Hou, Y.; Martens, W.; Mahmood, N.; Zhang, S. Microporous bamboo biochar for lithium-sulfur batteries. *Nano Res.* **2014**, *8*, 129–139. [[CrossRef](#)]
43. Xu, G.; Han, J.; Ding, B.; Nie, P.; Pan, J.; Dou, H.; Lia, H.; Zhang, X. Biomass-derived porous carbon materials with sulfur and nitrogen dual-doping for energy storage. *Green Chem.* **2015**, *17*, 1668–1674. [[CrossRef](#)]
44. Sun, Y.; Shi, X.L.; Yang, Y.L.; Suo, G.Q.; Zhang, L.; Lu, S.Y.; Chen, Z.G. Biomass-Derived Carbon for High-Performance Batteries: From Structure to Properties. *Adv. Funct. Mater.* **2022**, *32*, 2201584. [[CrossRef](#)]
45. Park, S.; Kim, J.; Kown, K. A review on biomass-derived N-doped carbons as electrocatalysts in electrochemical energy applications. *Chem. Eng. J.* **2022**, *446*, 137116. [[CrossRef](#)]
46. Yuan, H.D.; Liu, T.F.; Liu, Y.J.; Nai, J.W.; Wang, Y.; Zhang, W.K.; Tao, X.Y. A review of biomass materials for advanced lithium-sulfur batteries. *Chem. Sci.* **2019**, *10*, 7484. [[CrossRef](#)]
47. Liu, P.T.; Wang, Y.Y.; Liu, J.H. Biomass-derived porous carbon materials for advanced lithium sulfur batteries. *J. Energy Chem.* **2019**, *34*, 171–185. [[CrossRef](#)]
48. Li, Q.; Liu, Y.P.; Wang, Y.; Chen, Y.X.; Guo, X.D.; Wu, Z.G.; Zhong, B.H. Review of the application of biomass-derived porous carbon in lithium-sulfur batteries. *Ionics* **2020**, *26*, 4765–4781. [[CrossRef](#)]
49. Feng, Y.; Jiang, J.; Xu, Y.; Wang, S.; An, W.; Chai, Q.; Prova, U.; Wang, C.; Huang, G. Biomass derived diverse carbon nanostructure for electrocatalysis, energy conversion and storage. *Carbon* **2023**, *211*, 118105. [[CrossRef](#)]

50. Zhao, Z.Q.; Su, Z.; Chen, H.L.; Yi, S.; Zhang, W.Y.; Niu, B.; Zhang, Y.Y.; Long, D.H. Renewable biomass-derived carbon-based hosts for lithium–sulfur batteries. *Sustain. Energy Fuels* **2022**, *6*, 5211. [[CrossRef](#)]
51. Tian, X.H.; Yan, C.Z.; Kang, J.B.; Yang, X.Y.; Li, Q.X.; Yan, J.; Deng, N.P.; Cheng, B.; Kang, W.M. Working Mechanisms and Structure Engineering of Renewable Biomass-Derived Materials for Advanced Lithium-Sulfur Batteries: A Review. *ChemElectroChem* **2022**, *9*, e202100995. [[CrossRef](#)]
52. Senthil, C.; Lee, C.W. Biomass-derived biochar materials as sustainable energy sources for electrochemical energy storage devices. *Renew. Sustain. Energy Rev.* **2021**, *137*, 110464. [[CrossRef](#)]
53. Wang, Y.Z.; Huang, X.X.; Zhang, S.Q.; Hou, Y.L. Sulfur Hosts against the Shuttle Effect. *Small Methods* **2018**, *2*, 1700345. [[CrossRef](#)]
54. Walle, M.D. Environmental Solid Waste-derived Carbon for Advanced Rechargeable Lithium-Sulfur Batteries: A Review. *ChemistrySelect* **2022**, *7*, e202200511. [[CrossRef](#)]
55. Benitez, A.; Amaro-Gahete, J.; Chien, Y.C.; Caballero, A.; Morales, J.; Brandell, D. Recent advances in lithium-sulfur batteries using biomass-derived carbons as sulfur host. *Renew. Sustain. Energy Rev.* **2022**, *154*, 111783. [[CrossRef](#)]
56. Zhang, B.; Qin, X.; Li, G.R.; Gao, X.P. Enhancement of long stability of sulfur cathode by encapsulating sulfur into micropores of carbon spheres. *Energy Environ. Sci.* **2010**, *3*, 1531–1537. [[CrossRef](#)]
57. Ji, X.L.; Lee, K.T.; Nazar, L.F. A highly ordered nanostructured carbon-sulphur cathode for lithium-sulphur batteries. *Nat. Mater.* **2009**, *8*, 500–506. [[CrossRef](#)]
58. Liang, C.D.; Dudney, N.J.; Howe, J.Y. Hierarchically Structured Sulfur/Carbon Nanocomposite Material for High-Energy Lithium Battery Chemistry of Materials. *Chem. Mater.* **2009**, *21*, 4724–4730. [[CrossRef](#)]
59. Jung, D.S.; Hwang, T.H.; Lee, J.H.; Koo, H.Y.; Shakoor, R.A.; Kahraman, R.; Jo, Y.N.; Park, M.S.; Choi, J.W. Hierarchical porous carbon by ultrasonic spray pyrolysis yields stable cycling in lithium-sulfur battery. *Nano Lett.* **2014**, *14*, 4418–4425. [[CrossRef](#)]
60. Li, Z.; Jiang, Y.; Yuan, L.X.; Yi, Z.Q.; Wu, C.; Liu, Y.; Strasser, P.; Huang, Y.H. A highly ordered meso@microporous carbon-supported sulfur@smaller sulfur core-shell structured cathode for Li-S batteries. *ACS Nano* **2014**, *8*, 9295–9303. [[CrossRef](#)]
61. Chen, C.G.; Li, D.J.; Gao, L.; Harks, P.R.M.L.; Eichel, R.A.; Notten, P.H.L. Carbon-coated core-shell Li₂S@C nanocomposites as high performance cathode materials for lithium–sulfur batteries. *J. Mater. Chem. A* **2017**, *5*, 1428–1433. [[CrossRef](#)]
62. Yang, T.; Wang, X.L.; Wang, D.H.; Li, S.H.; Xie, D.; Zhang, X.Q.; Xia, X.H.; Tu, J.P. Facile and scalable synthesis of nanosized core-shell Li₂S@C composite for high-performance lithium–sulfur batteries. *J. Mater. Chem. A* **2016**, *4*, 16653–16660. [[CrossRef](#)]
63. Sun, Q.; He, B.; Zhang, X.Q.; Lu, A.H. Engineering of Hollow Core-Shell Interlinked Carbon Spheres for Highly Stable Lithium-Sulfur Batteries. *ACS Nano* **2015**, *9*, 8504–8513. [[CrossRef](#)]
64. Zhou, G.M.; Yin, L.C.; Wang, D.W.; Li, L.; Pei, S.F.; Gentle, I.R.; Li, F.; Cheng, H.M. Fibrous hybrid of graphene and sulfur nanocrystals for high-performance lithium-sulfur batteries. *ACS Nano* **2013**, *7*, 5367–5375. [[CrossRef](#)] [[PubMed](#)]
65. Zhou, G.M.; Li, L.; Ma, C.Q.; Wang, S.G.; Shi, Y.; Koratkar, N.; Ren, W.C.; Li, F.; Cheng, H.M. A graphene foam electrode with high sulfur loading for flexible and high energy Li-S batteries. *Nano Energy* **2015**, *11*, 356–365. [[CrossRef](#)]
66. Zhu, L.; Peng, H.J.; Liang, J.Y.; Huang, J.Q.; Chen, C.M.; Guo, X.F.; Zhu, W.C.; Li, P.; Zhang, Q. Interconnected carbon nanotube/graphene nanosphere scaffolds as free-standing paper electrode for high-rate and ultra-stable lithium–sulfur batteries. *Nano Energy* **2015**, *11*, 746–755. [[CrossRef](#)]
67. Song, J.X.; Gordin, M.L.; Xu, T.; Chen, S.R.; Yu, Z.X.; Sohn, H.; Lu, J.; Ren, Y.; Duan, Y.H.; Wang, D.H. Strong lithium polysulfide chemisorption on electroactive sites of nitrogen-doped carbon composites for high-performance lithium-sulfur battery cathodes. *Angew. Chem. Int. Ed. Engl.* **2015**, *54*, 4325–4329. [[CrossRef](#)]
68. Yang, C.P.; Yin, Y.X.; Ye, H.; Jiang, K.C.; Zhang, J.; Guo, Y.G. Insight into the effect of boron doping on sulfur/carbon cathode in lithium-sulfur batteries. *ACS Appl. Mater. Interfaces* **2014**, *6*, 8789–8795. [[CrossRef](#)]
69. Wang, N.N.; Xu, Z.F.; Xu, X.; Liao, T.; Tang, B.; Bai, Z.C.; Dou, S.X. Synergistically Enhanced Interfacial Interaction to Polysulfide via N,O Dual-Doped Highly Porous Carbon Microrods for Advanced Lithium-Sulfur Batteries. *ACS Appl. Mater. Interfaces* **2018**, *10*, 13573–13580. [[CrossRef](#)]
70. Chen, L.; Feng, J.R.; Zhou, H.H.; Fu, C.P.; Wang, G.C.; Yang, L.M.; Xu, C.X.; Chen, Z.X.; Yang, W.J.; Kuang, Y.F. Hydrothermal preparation of nitrogen, boron co-doped curved graphene nanoribbons with high dopant amounts for high-performance lithium sulfur battery cathodes. *J. Mater. Chem. A* **2017**, *5*, 7403–7415. [[CrossRef](#)]
71. Xu, J.; Su, D.W.; Zhang, W.X.; Bao, W.Z.; Wang, G.X. A nitrogen–sulfur co-doped porous graphene matrix as a sulfur immobilizer for high performance lithium–sulfur batteries. *J. Mater. Chem. A* **2016**, *4*, 17381–17393. [[CrossRef](#)]
72. Lee, J.; Oh, J.; Jeon, Y.; Piao, Y.Z. Multi-Heteroatom-Doped Hollow Carbon Attached on Graphene Using LiFePO₄ Nanoparticles as Hard Templates for High-Performance Lithium–Sulfur Batteries. *ACS Appl. Mater. Interfaces* **2018**, *10*, 26485–26493. [[CrossRef](#)] [[PubMed](#)]
73. Deng, J.; Li, M.; Wang, Y. Biomass-derived carbon: Synthesis and applications in energy storage and conversion. *Green Chem.* **2016**, *18*, 4824–4854. [[CrossRef](#)]
74. Wang, J.; Nie, P.; Ding, B.; Dong, S.; Hao, X.; Doua, H.; Zhang, X. Biomass derived carbon for energy storage devices. *J. Mater. Chem. A* **2017**, *5*, 2411–2428. [[CrossRef](#)]
75. Wu, D.P.; Liu, J.Y.; Chen, J.L.; Li, H.H.; Cao, R.G.; Zhang, W.C.; Gao, Z.Y.; Jiang, K. Promoting sulphur conversion chemistry with tri-modal porous N, O-codoped carbon for stable Li–S batteries. *J. Mater. Chem. A* **2021**, *9*, 5497. [[CrossRef](#)]
76. Li, Y.; Liu, W.L.; Li, S.L.; Meng, F.C.; Chen, Y.Z.; Wu, H.T.; Liu, J.H. From purple sweet potato to sustainable lithium-sulfur batteries. *Mater. Lett.* **2022**, *325*, 132893. [[CrossRef](#)]

77. Rojas, M.D.; Lobos, M.L.N.; Para, M.L.; María Quijón, E.G.; Cámara, O.; Barraco, D.; Moyano, E.L.; Luque, G.L. Activated carbon from pyrolysis of peanut shells as cathode for lithium-sulfur batteries. *Biomass Bioenergy* **2021**, *146*, 105971. [[CrossRef](#)]
78. Chen, H.W.; Xia, P.T.; Lei, W.X.; Pan, Y.; Zou, Y.L.; Ma, Z.S. Preparation of activated carbon derived from biomass and its application in lithium-sulfur batteries. *J. Porous Mater.* **2019**, *26*, 1325–1333. [[CrossRef](#)]
79. Lee, S.Y.; Choi, Y.J.; Kim, J.K.; Lee, S.J.; Bae, J.S.; Jeong, E.D. Biomass-garlic-peel-derived porous carbon framework as a sulfur host for lithium-sulfur batteries. *Ind. Eng. Chem. Res.* **2021**, *94*, 272–281. [[CrossRef](#)]
80. Chang, Y.G.; Ren, Y.M.; Zhu, L.K.; Li, Y.; Li, T.; Ren, B.Z. Preparation of macadamia nut shell porous carbon and its electrochemical performance as cathode material for lithium-sulfur batteries. *Electrochim. Acta* **2022**, *420*, 140454. [[CrossRef](#)]
81. Deng, Y.X.; Lei, T.Y.; Feng, Y.Y.; Zhang, B.; Ding, H.Y.; Lu, Q.; Tian, R.; Mushtaq, M.; Guo, W.J.; Yao, M.M.; et al. Biomass fallen leaves derived porous carbon for high performance lithium sulfur batteries. *Ionics* **2023**, *29*, 1029–1038. [[CrossRef](#)]
82. Yang, Y.; Yang, R.; Fan, C.J.; Huang, Y.; Yan, Y.L.; Zou, Y.M.; Xu, Y.H. Eucommia leaf residue-derived hierarchical porous carbon by KCl and CaCl₂ Co-auxiliary activation for lithium sulfur batteries. *Mater. Charact.* **2023**, *195*, 112522. [[CrossRef](#)]
83. Zhang, L.M.; Zhao, W.Q.; Yuan, S.H.; Jiang, F.; Chen, X.Q.; Yang, Y.; Ge, P.; Sun, W.; Ji, X.B. Engineering the morphology/porosity of oxygen-doped carbon for sulfur host as lithium-sulfur batteries. *J. Energy Chem.* **2021**, *60*, 531–545. [[CrossRef](#)]
84. Wen, X.Y.; Zhang, C.F.; Zhou, W.; Chen, H.; Xiang, K.X. Nitrogen/sulfur co-doping for biomass carbon foam as superior sulfur hosts for lithium-sulfur batteries. *Int. J. Energy Res.* **2022**, *46*, 10606–10619. [[CrossRef](#)]
85. Kim, J.K.; Choi, Y.J.; Jeong, E.D.; Lee, S.J.; Kim, H.G.; Chung, J.M.; Kim, J.S.; Lee, S.Y.; Bae, J.S. Synthesis and Electrochemical Performance of Microporous Hollow Carbon from Milkweed Pappus as Cathode Material of Lithium-Sulfur Batteries. *Nanomaterials* **2022**, *12*, 3605. [[CrossRef](#)] [[PubMed](#)]
86. Nurhilal, O.; Hidayat, S.; Sumiarsa, D.; Risdiana, R. Natural Biomass-Derived Porous Carbon from Water Hyacinth Used as Composite Cathode for Lithium Sulfur Batteries. *Renew. Energy* **2023**, *15*, 1039. [[CrossRef](#)]
87. Xue, M.Z.; Xu, H.; Tan, Y.; Chen, C.; Li, B.; Zhang, C.M. A novel hierarchical porous carbon derived from durian shell as enhanced sulfur carrier for high performance Li-S batteries. *J. Energy Chem.* **2021**, *893*, 115306. [[CrossRef](#)]
88. Xiao, Q.H.Q.; Li, G.R.; Li, M.J.; Liu, R.P.; Li, H.B.; Ren, P.F.; Dong, Y.; Feng, M.; Chen, Z.W. Biomass-derived nitrogen-doped hierarchical porous carbon as efficient sulfur host for lithium-sulfur batteries. *J. Energy Chem.* **2020**, *44*, 61–67. [[CrossRef](#)]
89. Ma, Z.W.; Sui, W.H.; Liu, J.; Wang, W.J.; Li, S.M.; Chen, T.T.; Yang, G.L.; Zhu, K.X.; Li, Z.J. Pomelo peel-derived porous carbon as excellent LiPS anchor in lithium-sulfur batteries. *J. Solid State Electrochem.* **2022**, *26*, 973–984. [[CrossRef](#)]
90. Wen, Y.T.; Wang, X.B.; Huang, J.Y.; Li, Y.; Li, T.; Ren, B.Z. Coffee grounds derived sulfur and nitrogen dual-doped porous carbon for the cathode material of lithium-sulfur batteries. *Carbon Lett.* **2023**. [[CrossRef](#)]
91. Liu, Y.; Lee, D.J.; Cho, K.K.; Zou, Y.M.; Ahn, H.J.; Ahn, J.H. Promoting long cycle life with honeycomb-like tri-modal porous carbon for stable lithium-sulfur polymer batteries. *J. Alloys Compd.* **2023**, *932*, 167704. [[CrossRef](#)]
92. Salimi, P.; Venezia, E.; Taghavi, S.; Tieuli, S.; Carbone, L.; Prato, M.; Signoretto, M.; Qiu, J.F.; Zaccaria, R.P. Lithium-Metal Free Sulfur Battery Based on Waste Biomass Anode and Nano-Sized Li₂S Cathode. *Energy Environ. Mater.* **2023**, e12567. [[CrossRef](#)]
93. Choi, J.R.; Kim, E.; Park, B.I.; Choi, I.; Park, B.H.; Lee, S.B.; Lee, J.L.; Yu, S. Meringue-derived hierarchically porous carbon as an efficient polysulfide regulator for lithium-sulfur batteries. *J. Ind. Eng. Chem.* **2022**, *115*, 355–364. [[CrossRef](#)]
94. Feng, L.J.; Lu, M.; Shen, W.N.; Qiu, X.Y. N/O dual-doped hierarchical porous carbon boosting cathode performance of lithium-sulfur batteries. *Mater. Express* **2022**, *12*, 337–346. [[CrossRef](#)]
95. Cui, J.Q.; Liu, J.; Chen, X.; Meng, J.S.; Wei, S.Y.; Wu, T.; Wang, Y.; Xie, Y.M.; Lu, C.Z.; Zhang, X.C. Ganoderma Lucidum-derived erythrocyte-like sustainable materials. *Carbon* **2022**, *196*, 70–77. [[CrossRef](#)]
96. Liang, J.F.; Xu, Y.Q.; Li, C.; Yan, C.; Wang, Z.W.; Xu, J.F.; Guo, L.L.; Li, Y.F.; Zhang, Y.G.; Liu, H.T.; et al. Traditional Chinese medicine residue-derived micropore-rich porous carbon frameworks as efficient sulfur hosts for high-performance lithium-sulfur batteries. *Dalton Trans.* **2022**, *51*, 129. [[CrossRef](#)]
97. Li, X.; Cheng, X.; Gao, M.; Ren, D.; Liu, Y.; Guo, Z.; Shang, C.; Sun, L.; Pan, H. Amylose-Derived Macrohollow Core and Microporous Shell Carbon Spheres as Sulfur Host for Superior Lithium-Sulfur Battery Cathodes. *ACS Appl. Mater. Interfaces* **2017**, *9*, 10717–10729. [[CrossRef](#)]
98. Li, J.; Qin, F.; Zhang, L.; Zhang, K.; Li, Q.; Lai, Y.; Zhang, Z.; Fang, J. Mesoporous carbon from biomass: One-pot synthesis and application for Li-S batteries. *J. Mater. Chem. A* **2014**, *2*, 13916. [[CrossRef](#)]
99. Zhong, Y.; Xia, X.; Deng, S.; Zhan, J.; Fang, R.; Xia, Y.; Wang, X.; Zhang, Q.; Tu, J. Popcorn Inspired Porous Macrocellular Carbon: Rapid Puffing Fabrication from Rice and Its Applications in Lithium-Sulfur Batteries. *Adv. Energy Mater.* **2018**, *8*, 1701110. [[CrossRef](#)]
100. Ren, G.; Li, S.; Fan, Z.-X.; Warzywodac, J.; Fan, Z. Soybean-derived hierarchical porous carbon with large sulfur loading and sulfur content for high-performance lithium-sulfur batteries. *J. Mater. Chem. A* **2016**, *4*, 16507–16515. [[CrossRef](#)]
101. Li, Q.; Liu, Y.P.; Yang, L.W.; Liu, Y.H.; Chen, Y.X.; Guo, X.D.; Wu, Z.G.; Zhong, B.H. N, O co-doped chlorella-based biomass carbon modified separator for lithium-sulfur battery with high capacity and long cycle performance. *J. Colloid Interface Sci.* **2021**, *585*, 43–50. [[CrossRef](#)] [[PubMed](#)]
102. Zhu, L.; Li, J.N.; Xie, H.B.; Shen, X.Q. Biomass-derived high value-added porous carbon as the interlayer material for advanced lithium-sulfur batteries. *Ionics* **2022**, *28*, 3207–3215. [[CrossRef](#)]
103. Wang, X.; Yang, L.W.; Li, R.; Chen, Y.X.; Wu, Z.G.; Zhong, B.H.; Guo, X.D. Heteroatom-doped Ginkgo Folium porous carbon modified separator for high-capacity and long-cycle lithium-sulfur batteries. *Appl. Surf. Sci.* **2022**, *602*, 154342. [[CrossRef](#)]

104. Guo, Y.C.; Chen, L.X.; Wu, Y.; Lian, J.L.; Tian, Y.; Zhao, Z.Y.; Shao, W.Y.; Ye, Z.Z.; Lu, J.G. Rotten albumen derived layered carbon modified separator for enhancing performance of Li-S batteries. *J. Electroanal. Chem.* **2021**, *895*, 115511. [[CrossRef](#)]
105. Shao, H.; Ai, F.; Wang, W.; Zhang, H.; Wang, A.; Feng, W.; Huang, Y. Crab shell-derived nitrogen-doped micro-/mesoporous carbon as an effective separator coating for high energy lithium–sulfur batteries. *J. Mater. Chem. A* **2017**, *5*, 19892–19900. [[CrossRef](#)]
106. Gu, X.; Lai, C.; Liu, F.; Yang, W.; Hou, Y.; Zhang, S. A conductive interwoven bamboo carbon fiber membrane for Li–S batteries. *J. Mater. Chem. A* **2015**, *3*, 9502–9509. [[CrossRef](#)]
107. Yang, J.; Chen, F.; Li, C.; Bai, T.; Longa, B.; Zhou, X. A free-standing sulfur-doped microporous carbon interlayer derived from luffa sponge for high performance lithium–sulfur batteries. *J. Mater. Chem. A* **2016**, *4*, 14324–14333. [[CrossRef](#)]
108. Wei, Y.B.; Cheng, W.H.; Huang, Y.D.; Liu, Z.J.; Sheng, R.; Wang, X.C.; Jia, D.Z.; Tang, X.C. P-Doped Cotton Stalk Carbon for High-Performance Lithium-Ion Batteries and Lithium–Sulfur Batteries. *Langmuir* **2022**, *38*, 11610–11620. [[CrossRef](#)]
109. Sabet, S.M.; Sapkota, N.; Chiluwal, S.; Zheng, T.; Clemos, C.M.; Rao, A.M.; Pilla, S. Sulfurized Polyacrylonitrile Impregnated Delignified Wood-Based 3D Carbon Framework for High-Performance Lithium–Sulfur Batteries. *ACS Sustain. Chem. Eng.* **2023**, *11*, 2314–2323. [[CrossRef](#)]
110. Liu, H.; Liu, W.L.; Meng, F.C.; Jin, L.Y.; Li, S.L.; Cheng, S.; Jiang, S.D.; Zhou, R.L.; Liu, J.H. Natural nori-based porous carbon composite for sustainable lithium-sulfur batteries. *Sci. China Technol. Sci.* **2022**, *65*, 2380–2387. [[CrossRef](#)]
111. Zhu, M.L.; Wu, J.; Li, S.Q. Flower-like Ni/NiO microspheres decorated by sericin-derived carbon for high-rate lithium-sulfur batteries. *Ionics* **2021**, *27*, 5137–5145. [[CrossRef](#)]
112. Moreno, N.; Caballero, Á.; Morales, J. Improved performance of electrodes based on carbonized olive stones/S composites by impregnating with mesoporous TiO₂ for advanced Li-S batteries. *J Power Sources* **2016**, *313*, 21–29. [[CrossRef](#)]
113. Pang, Q.; Kundu, D.; Cuisinier, M. Surface-enhanced redox chemistry of polysulphides on a metallic and polar host for lithium-sulphur batteries. *Nat. Commun.* **2014**, *5*, 4759. [[CrossRef](#)] [[PubMed](#)]
114. Luna-Lama, F.; Hernández-Rentero, C.; Caballero, A. Biomass-derived carbon/g-MnO₂ nanorods/S composites prepared by facile procedures with improved performance for Li/S batteries. *Electrochim. Acta* **2018**, *292*, 522–531. [[CrossRef](#)]
115. Wang, J.; Wu, L.; Shen, L. CoO embedded porous biomass-derived carbon as dual-functional host material for lithium-sulfur batteries. *J. Colloid Interface Sci.* **2023**, *640*, 415–422. [[CrossRef](#)] [[PubMed](#)]
116. Lama, F.L.; Caballero, Á.; Morales, J. Synergistic effect between PPy: PSS copolymers and biomass-derived activated carbons: A simple strategy for designing sustainable highperformance Li–S batteries. *Sustain. Energy Fuels* **2022**, *6*, 1568–1586. [[CrossRef](#)]
117. Chen, R.X.; Zhou, Y.C.; Li, X.D. Cotton-Derived Fe/Fe₃C-Encapsulated Carbon Nanotubes for High-Performance Lithium–Sulfur Batteries. *Nano Lett.* **2022**, *22*, 1217–1224. [[CrossRef](#)]
118. Zhong, M.; Sun, J.C.; Shu, X.Q.; Guan, J.D.; Tong, G.S.; Ding, H.; Chen, L.Y.; Zhou, N.; Shuai, Y. N, P, O-codoped biochar from phytoremediation residues: A promising cathode material for Li–S batteries. *Nanotechnology* **2022**, *33*, 215403. [[CrossRef](#)]
119. Tesio, A.Y.; Gómez-Camer, J.L.; Morales, J. Simple and sustainable preparation of non-activated porous carbon from brewing waste for high-performance lithium–sulfur batteries. *ChemSusChem* **2020**, *13*, 3439–3446. [[CrossRef](#)]
120. Benítez, A.; Márquez, P.M.; Martín, Á. Simple and Sustainable Preparation of Cathodes for Li–S Batteries: Regeneration of Granular Activated Carbon from the Odor Control System of a Wastewater Treatment Plant. *ChemSusChem* **2021**, *14*, 3915–3925. [[CrossRef](#)]
121. Páez Jerez, A.L.; Mori, M.F.; Flexer, V. Water Kefir Grains—Microbial Biomass Source for Carbonaceous Materials Used as Sulfur-Host Cathode in Li-S Batteries. *Materials* **2022**, *15*, 8856. [[CrossRef](#)] [[PubMed](#)]
122. Benítez, A.; Morales, J.; Caballero, Á. Pistachio Shell-Derived Carbon Activated with Phosphoric Acid: A More Efficient Procedure to Improve the Performance of Li–S Batteries. *Nanomaterials* **2020**, *10*, 840. [[CrossRef](#)] [[PubMed](#)]
123. Liu, L.Z.; Xia, G.H.; Wang, D. Biomass-derived self-supporting sulfur host with NiS/C composite for high-loading Li-S battery cathode. *Sci. China Technol. Sci.* **2023**, *66*, 181–192. [[CrossRef](#)]
124. Lama, F.L.; Marangon, V.; Caballero, Á. Diffusional Features of a Lithium-Sulfur Battery Exploiting Highly Microporous Activated Carbon. *ChemSusChem* **2023**, *16*, e202202095. [[CrossRef](#)] [[PubMed](#)]
125. Liu, L.Z.; Xia, G.H.; Wang, D. Self-supporting Biomass Li–S Cathodes Decorated with Metal Phosphides—Higher Sulfur Loading, Better Stability, and Longer Cycle Life. *ACS Appl. Energy Mater.* **2022**, *5*, 15401–15411. [[CrossRef](#)]

Disclaimer/Publisher’s Note: The statements, opinions and data contained in all publications are solely those of the individual author(s) and contributor(s) and not of MDPI and/or the editor(s). MDPI and/or the editor(s) disclaim responsibility for any injury to people or property resulting from any ideas, methods, instructions or products referred to in the content.